

Review

Cite this article: Pandey S *et al* (2020). Ladakh: diverse, high-altitude extreme environments for off-earth analogue and astrobiology research. *International Journal of Astrobiology* **19**, 78–98. <https://doi.org/10.1017/S1473550419000119>

Received: 22 January 2019
Revised: 24 April 2019
Accepted: 6 May 2019
First published online: 13 June 2019

Key words:
analogue; astrobiology; high-elevation; hot-springs; India; Ladakh; permafrost

Author for correspondence:
Siddharth Pandey, E-mail: spandey@mum.amity.edu

Ladakh: diverse, high-altitude extreme environments for off-earth analogue and astrobiology research

Siddharth Pandey^{1–3}, Jonathan Clarke^{1,4}, Preeti Nema³, Rosalba Bonaccorsi^{5,6}, Sanjoy Som³, Mukund Sharma⁷, Binita Phartiyal⁷, Sudha Rajamani⁸, Rakesh Mogul^{3,9}, Javier Martin-Torres^{10,11}, Parag Vaishampayan³, Jennifer Blank^{3,5}, Luke Steller⁴, Anushree Srivastava¹², Randheer Singh⁷, Savannah McGuirk^{1,13}, María-Paz Zorzano^{10,14}, Johannes Milan Güttler¹⁰, Teresa Mendaza¹⁰, Alvaro Soria-Salinas¹⁰, Shamim Ahmad⁷, Arif Ansari⁷, Veeru Kant Singh⁷, Chaitanya Mungji⁸ and Niraja Bapat⁸

¹Mars Society Australia, Clifton Hill, Victoria, Australia; ²Amity Centre of Excellence in Astrobiology, Amity University Mumbai, Mumbai, India; ³Blue Marble Space Institute of Science, Seattle, Washington, USA; ⁴Australian Centre of Astrobiology, University of New South Wales, Sydney, New South Wales, Australia; ⁵Space Sciences Division, NASA Ames Research Center, Moffett Field, California, USA; ⁶SETI Institute, Carl Sagan Center, Mountain View, California, USA; ⁷Birbal Sahni Institute of Palaeosciences, Lucknow, India; ⁸Indian Institute of Science Education and Research, Pune India; ⁹California Polytechnic University, Pomona, California, USA; ¹⁰Department of Computer Science, Electrical and Space Engineering, Luleå University of Technology, Luleå, Sweden; ¹¹Instituto Andaluz de Ciencias de la Tierra (CSIC-UGR), Armilla, Granada, Spain; ¹²The Mars Society, Lakewood, Colorado, USA; ¹³Fenner School of Environment and Society, Australian National University, Australian Capital Territory, Australia and ¹⁴Centro de Astrobiología (INTA-CSIC), Torrejón de Ardoz, Madrid, Spain

Abstract

This paper highlights unique sites in Ladakh, India, investigated during our 2016 multidisciplinary pathfinding expedition to the region. We summarize our scientific findings and the site's potential to support science exploration, testing of new technologies and science protocols within the framework of astrobiology research. Ladakh has several accessible, diverse, pristine and extreme environments at very high altitudes (3000–5700 m above sea level). These sites include glacial passes, sand dunes, hot springs and saline lake shorelines with periglacial features. We report geological observations and environmental characteristics (of astrobiological significance) along with the development of regolith-landform maps for cold high passes. The effects of the diurnal water cycle on salt deliquescence were studied using the ExoMars Mission instrument mockup: HabitAbility: Brines, Irradiance and Temperature (HABIT). It recorded the existence of an interaction between the diurnal water cycle in the atmosphere and salts in the soil (which can serve as habitable liquid water reservoirs). Life detection assays were also tested to establish the best protocols for biomass measurements in brines, periglacial ice-mud and permafrost melt water environments in the Tso-Kar region. This campaign helped confirm the relevance of clays and brines as interest targets of research on Mars for biomarker preservation and life detection.

Introduction

Terrestrial analogues for off-Earth environments provide a natural laboratory for conducting experiments and testing instruments and operational practices for future space exploration missions. In addition to well-known analogue regions (Hipkin *et al.*, 2013), efforts are being made to recognize unexplored and less studied parts of the world and introduce relevant sites to the astrobiology community (Preston and Dartnell, 2014). The objective of this paper is to introduce Ladakh, India (Fig. 1), as a region of astrobiological significance by providing an overview of sites visited in August 2016. Ladakh is a cold, very high-altitude (~3000–5700 m above sea level; Fig. 2) Himalayan desert region located in the eastern part of the state of Jammu and Kashmir of Northern India. It offers a natural setting where a diverse range of mostly near-pristine extreme environments including glacial deposits, arid regions, dune fields and intra dune ponds, hot springs, saline lakes and permafrost regions can be found and accessed by road (1–2 days by car) from its capital city of Leh. Leh is directly accessible using commercial air carriers from Indira Gandhi International airport in Delhi. As a result of altitude, the region has lower atmospheric oxygen partial pressures, higher levels of UV irradiation and receives little to no rainfall. Such a rare setting is desirable for multidisciplinary astrobiology teams studying paleoenvironments, geobiology and those developing and testing

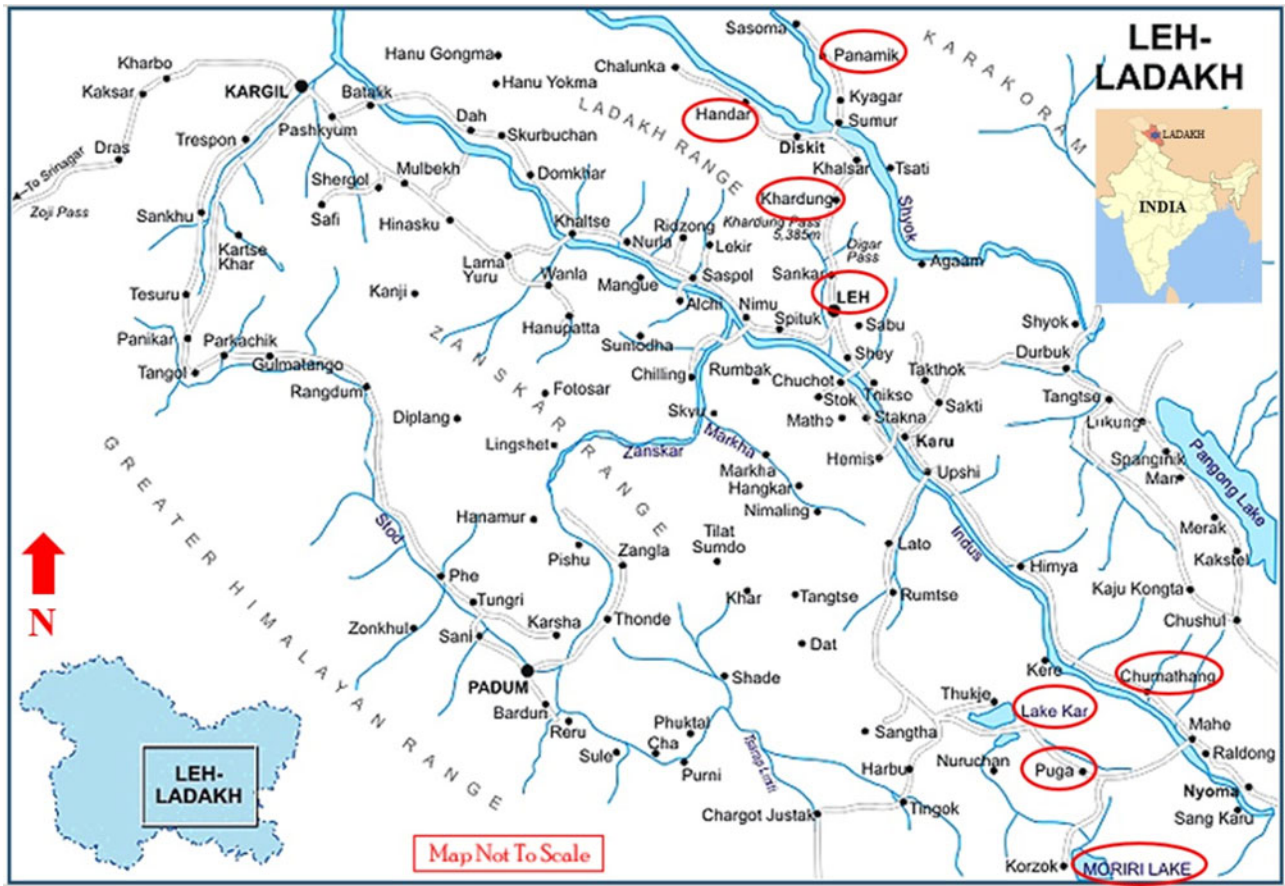


Fig. 1. Map of Ladakh, India visited sites circled in red (Image Courtesy: www.ladakh tours.com/ladakhmap.html).

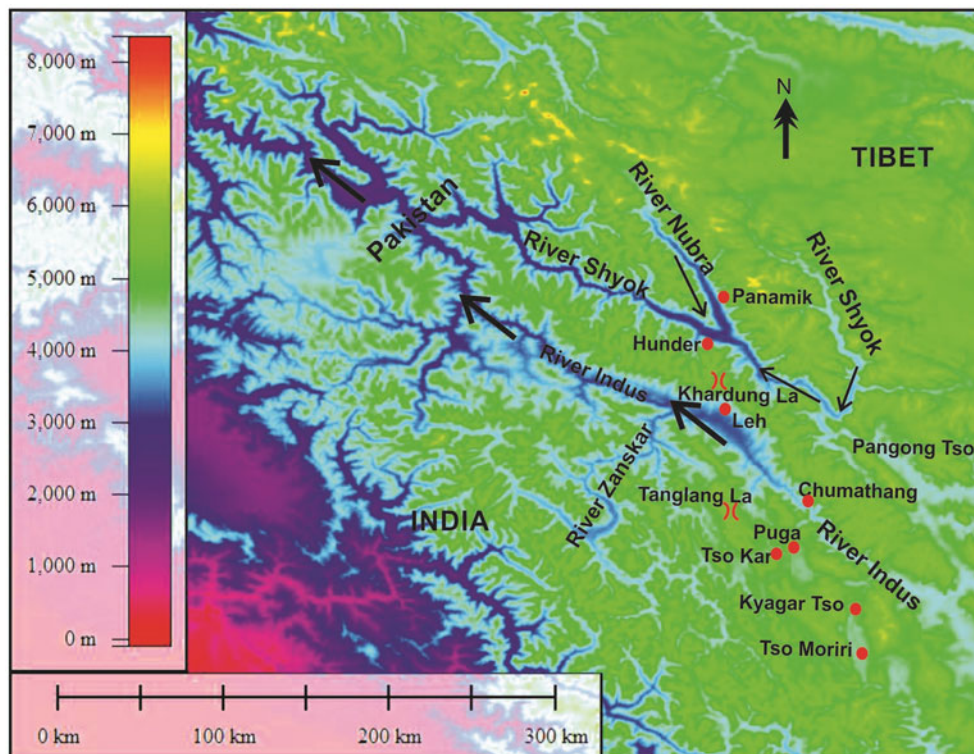


Fig. 2. Digital elevation model of the area (modified from Phartiyal *et al.*, 2014).

Table 1. Location type, elevation and coordinates of the expedition sites

Site	Type	Elevation (m above sea level)	Latitude, Longitude
Khardung La	Glacial deposit, high pass	5359	34°16'46.78"N, 77°36'13.70"E
Panamik	Hot springs	3206	34°46'52.80"N, 77°32'28.32"E
Hunder	Sand Dunes, Ephemeral ponds	3095	34°34'24.14"N, 77°29'49.89"E
Chumathang	Hot springs	3944	33°21'38.66"N, 78°20'35.33"E
Kyagar Tso	Alkaline Brine Lake	4700	33°06'26.14"N, 78°18'4.66"E
Puga	Hot springs	4414	33°13'39.38"N, 78°18'22.98"E
Tso-Kar	Alkaline Brine Lake, Permafrost	4535	33°18'56.63"N, 77° 57'20.30"E
Taglang La	Glacial deposit, high pass	5328	33°30'30.66"N, 77°46'17.19"E

Table 2. To highlight the 'astrobiological relevance' of the region, a list of activities is presented against the sites covered in the 2016 pathfinding expedition

Site Types →	Glacial High Passes		Sand Dunes and Ponds	Hot Springs			Saline Lake	Permafrost
	Khardung La	Taglang La	Hunder	Pa*	Ch*	Pu*	Sumdo	Tso Kar
Regolith Landform Mapping	X	X	•	•	•	•	•	•
Comparative Planetology	X	X	X	X	X	X	X	X
Instrument Testing (HABIT-ExoMars 2020)	X	X	X	•	•	•	X	X
Life Detection Analytical Protocols (ATP +LPS)	•	X	X	X	X	•	X	X
Biomass Distribution	•	X	X	X	X	•	X	X
Microbial Diversity / Metabolism	•	•	•	X	X	X	•	•

* Pa: Panamik, Ch: Chumathang, Pu: Puga
 X Done
 • Future Work

life detection techniques and instrumentation for other worlds. Our expedition was principally a scouting expedition to the region (covered sites listed in Table 1). As a result, we focus on describing geological settings and gathering environmental data of the sites, while also investigating their level of accessibility and pristineness.

Astrobiologically relevant sites

The visited sites are introduced section-wise with a brief overview of the previous investigations in the region, the geological setting and our observations describing the site's potential to support astrobiology research. A summary of the investigations conducted at some of the site types (glacial high passes, sand dunes and hot springs) is given. The relevant activities carried out per site (landform mapping, comparative planetology, instrument testing, life detection protocol study, biomass distribution, metabolism study) is presented in a table (Table 2) to bring out the 'astrobiology relevance' of the sites.

Glacial high passes

The high passes of Khardung La and Taglang La crest at altitudes of 5359 and 5328 m, respectively. Although the two passes have

similar altitude, their geomorphology and geology are very different. These high passes are unique in their high altitude, with rocks exposed to higher UV-A doses (~10× greater than sea level; Dvorkina and Steinberger, 1999), melt water pools at glacier terminuses and the presence of permafrost. These high passes present several analogue features for early Mars, given their combination of low atmospheric pressure, high UV (greater UV-A doses than experienced on Mars in the present day; Cockell *et al.*, 2000), permafrost, active periglacial activity, glaciers and glacier melt. The atmospheric density at 5300 m is approximately 0.64 kg m⁻³, compared with 1.2 kg m⁻³ at sea level. Hesperian Mars is estimated to have had an atmospheric density of at least 0.4 kg m⁻³ (Manga *et al.*, 2012). Noachian pressures may have been much higher (Cockell *et al.*, 2000). Preservation of biomarkers is another avenue of research in these high passes. Indeed, taphonomic pathways involved in the preservation of organic matter in these environments could help inform the preservation potential of biomarkers in soils, sediments and weathering profiles on early Mars. Such information is relevant for future Mars exploration instrumentation.

Site description

Khardung La Pass. Khardung La has been strongly eroded by glacial activity to the north and south, with steep U-shaped glacial

valleys eroded into the granites of the Ladakh batholiths (late Cretaceous–Palaeocene epoch, Weinberg *et al.*, 2000). The glacier on the south side is the Khardung glacier, while the smaller glacier and glacial remnants on the north and west sides (Fig. 3(a)) are unnamed. The pass itself is formed by a col, with the ridge east and west steepened by erosion into arêtes. The slopes are mantled by large blocks, forming a thick mantle talus. Down slope movement of the blocks is a frequent occurrence, lubricated by snow melt. The informally-named north Khardung glacier has a prominent recent moraine. Relatively flat surfaces in the valley floor to the north of the pass show development of polygonal ground and stone stripes, interspersed with the oriented boulders of block streams (Fig. 3(b) and (c)). One moraine (34°17.321'N, 77°35.714'E; altitude: 5098 m) possesses patterned ground, a typical characteristic feature of periglacial regions. This pattern is developed due to alternate freezing and thawing of the soil. The sides of the valley towards the locality known as North Pulu show well-developed talus cones of probable periglacial origin, while the valley floor, currently occupied by the headwaters of the Khardung Rong stream, shows a succession of terminal moraines. Age of deglaciation is unclear, however, the lake sediments in the valleys date post the Last Glacial Maximum (LGM) and the pro-glacial lake sediments date around Mid Holocene (Phartiyal *et al.*, 2013; Nag and Phartiyal, 2015; Phartiyal *et al.*, 2016). Features of potential astrobiological interest of Khardung La would include the rock surfaces exposed to a high UV flux and melt water pools at the terminus of the north Khardung glacier. Permafrost is likely to occur at a shallow depth throughout Khardung La (with layers at least 40 cm deep) by analogy with Chang La pass (5360 m, Pant *et al.*, 2005). However, the very coarse nature of the surface mantle and the shallow bedrock would make it difficult to access.

Taglang La. The bedrock at Taglang La is composed of metamorphosed sediments. The landscape is less steep than Khardung La, though still composed of the U-shaped valleys characteristic of glacial erosion (Fig. 4(a)). The smooth slopes suggest that the entire area was overridden by glacial ice in the past. Higher altitude glacial remnants are preserved at elevations of 5600 m, 2.5 km to the southwest of the pass. The pass occurs near the contact between two different rock types, carbonaceous phyllites and fine-grained quartzites to the west and coarse-grained white marbles to the east (Fig. 4(b)). The contact between the two lithologies runs almost north-south through the pass. The phyllites and quartzites are exposed only in roadside cuttings whereas the marbles form prominent knolls and steep-sided peaks. Fuchs and Linner (1995) date these sediments as Palaeozoic, possibly Permian. The regolith mantle over the phyllites is largely continuous, consisting of poorly sorted silt-to-pebble sized fragments and occasional large boulders of quartz, which are possible glacial erratics. The regolith is both riled and terraced, probably by runoff and solifluction, respectively. The regolith mantle over the marbles is discontinuous, with extensive areas of bare rock. Where present it consists of coarse sand to gravel-sized carbonate fragments.

Features of potential astrobiological interest at Taglang La would include the exposed rock surfaces, with the added contrast between the metamorphic fine-grained sediments and carbonates. Permafrost is also likely to occur at a shallow depth throughout Taglang La by analogy with Chang La (Pant *et al.*, 2005), and the very finer-grained nature of surface mantle may make access via surface excavation more practical than at Khardung La.

West-facing shadowed areas in road cuts below the pass are marked by well-developed icicles. Permafrost is likely very close to the surface.

Development of regolith-landform maps for glacial high passes

Regolith-landform mapping is an approach to describing the Earth's surface in terms of both landforms and the surface materials. These could include transported material, weathered rocks, duricrust, or fresh bedrock (Pain *et al.*, 2007; Pain, 2008). Techniques of regolith-landform mapping have proved an important part of any field study on Earth involving surface materials, landscape, biota and hydrology. The methodology can be extended to Mars analogue locations, and to the interpretation of Mars surface features (Clarke and Pain, 2004). Regolith-landform mapping methodologies have not previously been applied to regolith and landforms of terrestrial cold climates. Ladakh provided an opportunity to develop such a methodology. An example of regolith-landform mapping in a cold climate is shown in Fig. 5. Figure 5(a) shows an interpreted ground-level image of a steep, glacier-headed valley not far from Khardung La, and Fig. 5(b) is an interpreted Google Earth image of the same area. The units are consistent with each other. Each unit consists of regolith defined by a single landform and is a homogeneous composition at the scale of mapping. Regolith-landform units are characterized by three properties: a landform descriptor in lower case letters forming a prefix, a regolith material descriptor in upper case letters with lower case letters in brackets to describe interstitial ices, salts and carbonates (if present) and a numerical modifier for periglacial modification (if present) as a suffix. Each descriptor is unique. The units in Fig. 5 are described in Table 3. Results from the regolith mapping exercise are still being integrated with data from elsewhere. However, the results from the ground mapping at Khardung La closely match those made from aerial photographs and show the utility of the technique in the characterization of landforms and regolith materials in periglacial environments. One limiting factor identified in the methodology was in the use of aerial or satellite images in that the regolith materials could not be accurately predicted where there was a significant change in texture just below the resolution of the imagery. A prime example of this is the south-facing rock glaciers in the valley between Tso-Kar and Puga, the surface of these appears relatively smooth in Google Earth images, apart from furrows and ridges and occasional large boulders. Those examined on the ground, however, were largely covered by boulders that were smaller than the image resolution (0.7 m).

Deliquescent melting of calcium chloride at Khardung La

One of the goals of the campaign was to validate, in a representative environment, the operation of the HabitAbility: Brines, Irradiance and Temperature (HABIT) instrument. HABIT is part of the ExoMars Surface Platform of the European Space Agency (ESA) and the Russian Federal Space Agency (Roscosmos). HABIT is a cutting-edge, multipurpose instrument composed of: (i) ENVPACK, a surface environmental package devoted to evaluating the habitability of the landing site; and (ii) BOTTLE (Brine Observation Transition To Liquid Experiment), an In-situ Resource Utilization instrument for future Mars exploration. The goal of the field-site validation was to demonstrate the basic functional principle of HABIT for liquid brine production, namely the water absorption from the atmosphere on salt support. Other goals were to validate the time response of the salts to ambient conditions, the efficiency of air flow through the



Fig. 3. (a) Snout of the small glacier, west of Khardung La. (b) Sorted margin of the stone polygon in the alpine meadow to north of Khardung La. (c) Coring soils in the alpine meadow, north of Khardung La. (Photo credits: Dr Jonathan Clarke).

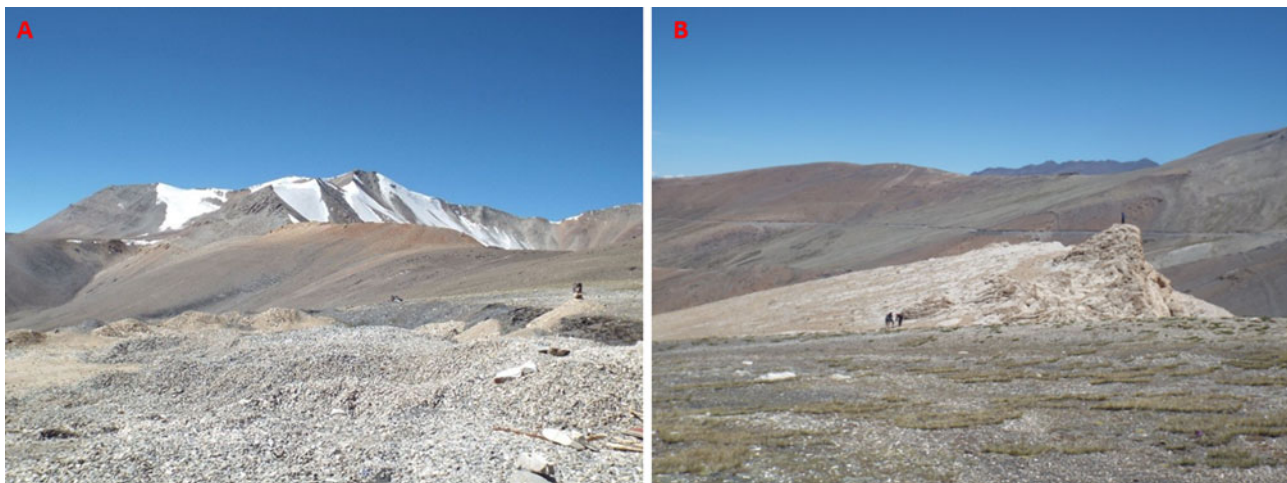


Fig. 4. (a) View from Taglang La looking south. (b) North-facing slope at Taglang La showing the contrast between dark-toned quartz-rich regolith on carbonaceous sediment in the foreground and barren, light-toned carbonaceous (limestone) outcrops in the background. Moss colonized terracettes and solifluction lobes visible in the foreground (Photo credits: Dr Jonathan Clarke).

HABIT-lid and the role of the lid in shadowing and protecting the salts, and the phase change of non-conducting salts to conducting hydrates and then to liquid brine. Figure 6 shows an open view of the HABIT field-site prototype. Both parts were covered by lids, except for vessel 6 of the BOTTLE container unit. Vessels 1 and 2 were filled with sodium perchlorate, vessels 3 and 4 were filled with calcium perchlorate and vessels 5 and 6 were filled with calcium chloride salts. Models can predict what the state of the salt is

in, assuming equilibrium with the atmosphere and under a given set of ambient temperature (T) and relative humidity (RH). The phase diagram of each tested salt can be used to interpret the change of conductivities, depending on the measured RH and T values, at each one of the measured sites. The ambient conditions at different sampled sites are shown in Fig. 7 against the phase diagram of calcium chloride. Figure 8 shows an example of the HABIT measurements at Khardung La, here shown only for

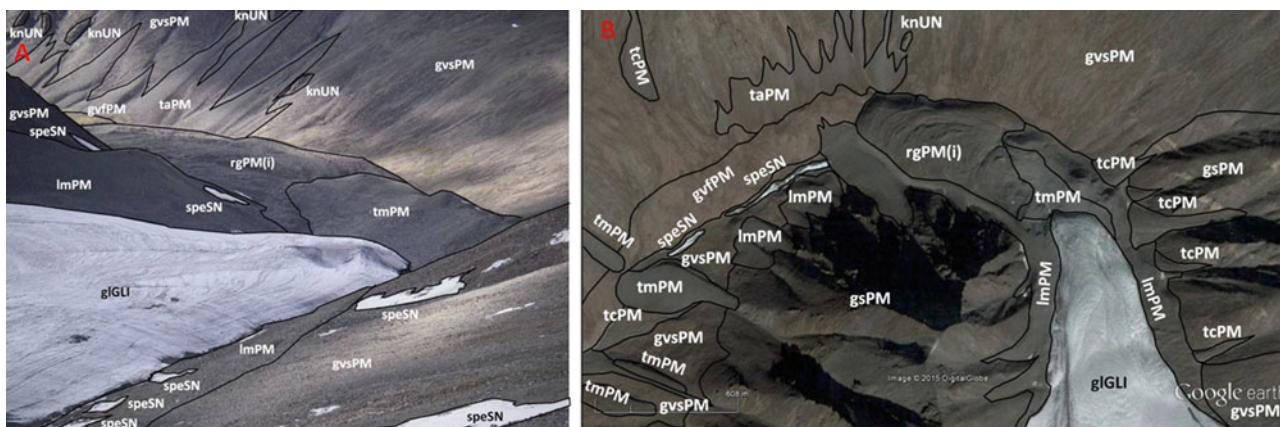


Fig. 5. (a) Site-scale regolith-landform units mapped onto a ground-level photograph from Phyang glacier terminus, Ladakh. (b) Regolith-landform map of the Phyang glacier in Ladakh on Google Earth base image. Location 34°17'33.66"N, 77°33'12.69"E (Image credits: Dr Jonathan Clarke).

Table 3. Units and definitions for regolith-landform maps in Fig. 5(a) and (b)

Units	Definition
gvfPM	Glacial valley floor, polymict materials
gvsPM	Glacial valley side polymict materials
gGLI	Glacier, glacial ice
lmPM	Lateral moraine, polymict materials
knUN	Knob, undifferentiated materials
rgPM(i)	Rock glacier, polymict materials, ice cemented
speSN	Snow patch, seasonal snow
taPM	Talus apron, polymict materials
tcPM	Talus cone, polymict materials
tmPM	Terminal moraine, polymict materials

calcium chloride. The conductivity of a salt solution requires AC (alternating current) excitation, to avoid the polarization of the solution and the corrosion of the electrodes. Additionally, the AC current needs to operate at high frequencies since a salt solution behaves like a resistance + capacitor circuit. For this specific case, the prototype of HABIT operates, with a square wave of 5 V amplitude, at 10 kHz. Previous measurements of electrical conductivity on Mars by the Thermal and Electrical Conductivity Probe (TECP) of the Phoenix lander were implemented similarly, with a square wave running at 1 kHz and an input voltage of 2.5. These environmental measurements informed that at Khardung La, environmental conditions were such that calcium chloride should hydrate and then melt into the liquid phase by deliquescence.

Sand dunes

Aeolian features are common in Ladakh, especially along valley floors and the lee side of lakes where there are locally abundant supplies of sand-sized materials. Landforms include dunes (Pant *et al.*, 2005) and sand ramps (Kumar *et al.*, 2016), and sand sheets associated with lakes such as Kyagar Tso (Section 'Kyagar Tso'). The expedition team carried out several investigations at the Hunder dunes where the dunes provide useful analogues for

small Martian valley dunes and the ephemeral pools in the swales and their deposits may be of astrobiological interest as similar pools could have conceivably existed on early Mars during the Noachian or even later during Martian history (e.g. Howard *et al.*, 2005). Ancient inter-dune pools on Earth have been known to preserve fossils such as stromatolites (Eisenberg 2003). Similar deposits should be recognizable in ancient dune deposits on Mars and may preserve signs of ancient life. These features enhance the potential of this site as a test bed for astrobiology-relevant investigations.

Hunder dunes: site description and observations

The dunes at Hunder, with their short-lived pools and fluvial sediments in the inter-dune spacings (Fig. 9(a) and (d)), are easily accessible for exploration and sampling. These, along with other dunes in the Shyok and Nubra valleys (Fig. 2), are largely unstudied. Exposed rocks are categorized under the Shyok Group (Thakur, 1981), Tsoltak and Shyok Formation (Thanh *et al.*, 2010), and Shyok Formation (Weinberg *et al.*, 2000; Kumar *et al.*, 2016). Dortch *et al.*, 2010 describe glacially derived landforms, e.g., moraines and roche moutonnées around the area, formed during the Deskit 1 and Deskit 2 glacial stages. The rapidly declining elevation of these landforms near the Hunder village is considered an indicator for the termination of glacial ice. Pant *et al.* (2005) reported that the dune fields are the only Quaternary deposits that can be observed downstream of the River Shyok. All these dunes are probable results of climatic events during Holocene time. However, Phartiya and Sharma (2009) describe the whole area as having once existed under a massive lake system which extended for ~40–50 km upstream and into the Nubra valley during late Quaternary. The Hunder dune field lines the south-western side of the Shyok valley between Diskit and Hunder. Each of these towns is situated atop a large alluvial fan, which acts to shelter the dune field from intense winds blowing up or down the valley. The dune field consists of three distinct areas, separated by a freshwater creek and an anabranch of the River Shyok. Rippled sedimentary deposits indicate that water has flowed over the dune field site at some time. However, the timeframe of these events is unclear. Construction of rose diagrams using QGIS software indicated a seasonal trend in dune orientation and wind direction, unusual for barchan, transverse or barchanoid dunes but can be explained

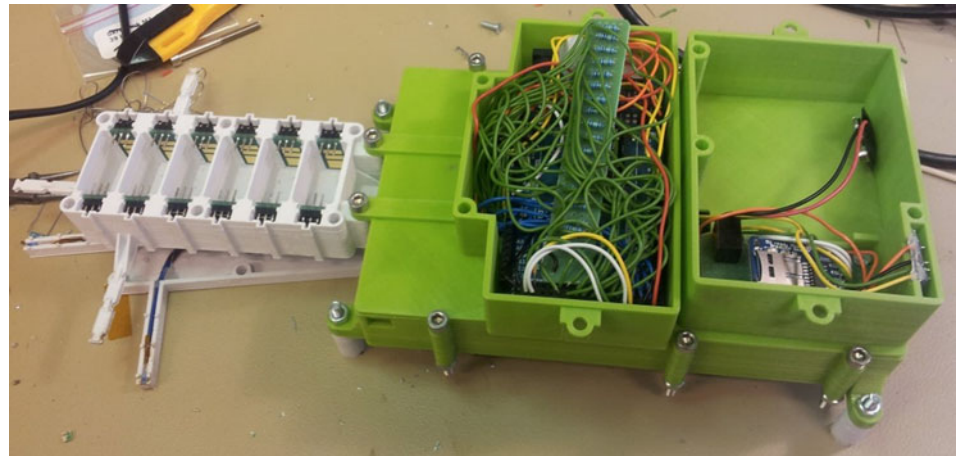


Fig. 6. Open view of the HABIT prototype for the field-site campaign, including the six vessels of the BOTTLE container unit (in white), with the conductivity pins at three different heights and the electronic unit (in green) (Photo credit: HABIT team/LTU).

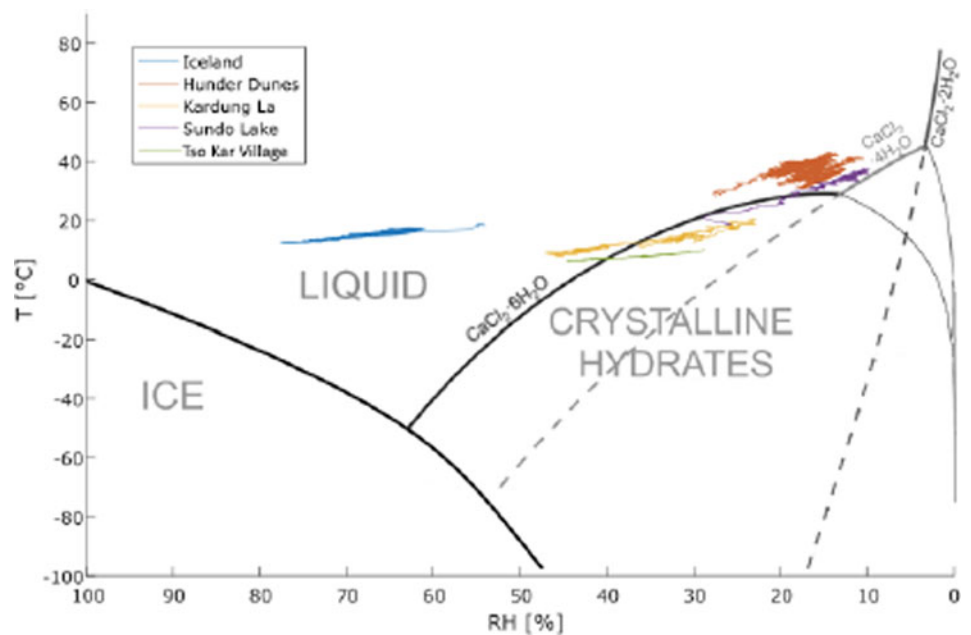


Fig. 7. Phase diagram of calcium chloride and measured ambient conditions in Ladakh compared to measurements taken in Iceland. The ambient conditions at Khardung La are clearly compatible with a transition from crystalline hydrated phase to liquid brine phase.

by the mild weather variation in the region, with the wind direction changing within 60° (McGuirk *et al.*, 2018).

Transverse-barchanoid dunes at Hunder indicate a consistent north-westerly wind direction. Many dunes in the westerly area of the dune field have a steep slip face with angles up to 35° recorded (equivalent to the angle of repose of loose sand). A variety of inter-dune surfaces including rocky ridges, layered sand swales and mud-cracked clays are present. These are shifting dunes due to wind funnel activity in this region. Recently, they have become very sparse but many are found on the left bank of the wide confluence (~10 km) of the Shyok and the Nubra rivers. Inter-dune ponds of small-to-moderate size mark hollows between some dunes. One of the ponds most closely examined was 20 cm deep at the deepest point and situated 2–3 m above the level of the creek. Some swale deposits have been inverted by aeolian erosion, exposing stacked cycles of fluvial and pond sediments capped by mud-cracked horizons. The age of these sediments is not known, but they are presumed to be from the Holocene. Hunder's ephemeral ponds (pH 6.0–6.5) (Fig. 9(b)) are an intriguing Mars analogue site for the study of clay

formation in a relatively dry, and relatively small dune field environment, accessible on foot. The ponds can be different with respect to vegetation distribution, depth and relationship with the surrounding clay beds. Some of the ponds contain clear water with more suspended particles, due to organic enrichment from plant debris and local fauna visitation when water becomes available. No recent river sand or flood deposits are apparent around the ponds, indicating the pond water is likely sustained by a high groundwater table, and/or recharging by rainstorms. It is likely that the ponds are recharged by rainwater seeping through the sand and collected over non-permeable beds of clay sediments.

The Hunder dune field could represent a suitable analogue model for understanding a desiccating early Mars (Fig. 9(c)), perhaps punctuated by short-lived liquid water, still supporting ephemeral life. Hunder's dry climate is ideal to assess how absorption and preservation of organic matter in clays could be related to the putative preservation potential of organics in Martian clay beds (e.g., Hamilton *et al.*, 2008). On Earth as well as on Mars, the reactivity between regolith's minerals and organics

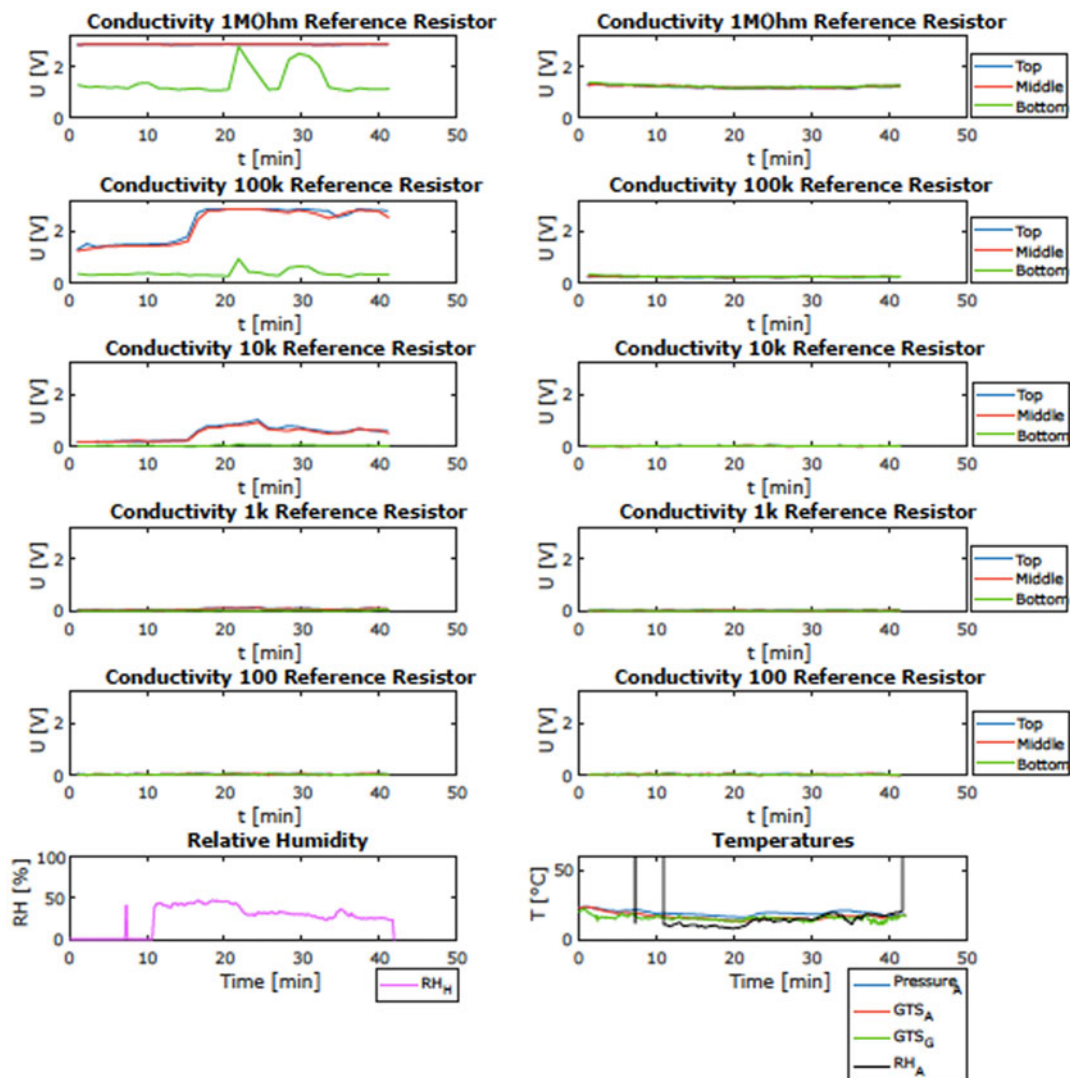


Fig. 8. Example of the observations of HABIT prototype at Khardung-La: change of electrical conductivity over time (shown in volts) for the CaCl_2 containers and the corresponding ambient RH and T. Here example of the signal observed in the calcium chloride samples of a covered-compartment (left) and an open-air compartment (right) and simultaneous ambient temperature and RH.

affects preservation and detection of organic matter and thus the direct evidence of life (e.g., Klein *et al.*, 1976; Navarro-González *et al.*, 2010). Organics are poorly preserved in oxidising environments (Davila *et al.*, 2011), but can be preserved in clay-rich deposits against oxidation (e.g., Hedges and Keil, 1995). Dissolved organics adsorbed on mineral surfaces can be preserved against microbial decay (e.g., Aggarwal *et al.*, 2006; Yu *et al.*, 2009). Therefore, Hunder, akin to Martian dune fields and interdune clay deposits, could represent an intriguing target to seeking mineral, sedimentary and preserved molecular evidence of life.

Hot springs

Hot springs serve as valuable off-Earth analogue sites due to the presence of extreme conditions for the survival of life. These include high temperatures, extremes of pH, the paucity of dissolved oxygen and limited nutrients. Although not conducive for most of the life forms, hot springs host diverse microbial communities. Studies of these extremophilic microorganisms help understand adaptations of life to extreme environments that

may have relevance to the early Earth and Mars. The hot springs in Ladakh are potentially unique study sites for astrobiological research because of their high elevation. The regional geology comprises three tectonic belts. The Northern Belt consists of the Indus Group sedimentary sequence and the Ladakh granites, and hosts the Chumathang geothermal system (Craig *et al.*, 2013). The Central Belt consists of the Indus Suture Zone (ISZ), an area subjected to intense tectonic activity and uplift. The Southern Belt, containing the Puga Formation, is a succession of sedimentary and metasedimentary units consisting of Precambrian paragneiss, schist and phyllites, with interbedded layers of limestone and sections of locally intrusive Tertiary granites (Singh *et al.*, 2005). Because Ladakh lies in the rain shadow region of the Great Himalayas, the geochemistry of these hot springs is minimally influenced by atmospheric precipitation. These springs consist of moderately hot to very hot water (60–75°C; water boils at temperature 90°C at 3000 m altitude and 86°C at 4500 m altitude) of moderately alkaline pH (<9). The presence of calcium sulphates at some Ladakh springs suggests an analogy to primitive Martian environment where gypsum has been detected (Squyres *et al.*,



Fig. 9. (a) Wind eroded inter-dune sediments in Hunder (Photo Credit: Dr Jonathan Clarke). (b) Inter-dune Pond, Hunder (Photo Credit: Dr Jonathan Clarke). (c) For comparison, a dune field inside Endurance crater on Mars (Photo credit: Opportunity rover NASA/JPL Caltech). (d) Stack inverted dune swale deposits (Photo Credit: Dr Jonathan Clarke).



Fig. 10. (a) Panamik Hot Spring site. (b) Differing colouration of the biomass at hot spring source and along the flow (Photo Credits: Mr Rakesh Rao and Dr Mukund Sharma).

2004) and may help unravel putative Martian geomicrobiological processes (Shukla *et al.*, 2017).

Site description

Panamik springs. The Panamik area (Fig. 10) exposures rocks of the Karakoram Plutonic Complex (Thakur, 1981) including granites, granodiorites and leucogranites. In these rocks, various

minerals such as plagioclase, quartz, biotite, amphiboles, along with accessory magnetite, chalcopyrite, galena and zircon are reported (Thanh *et al.*, 2010). The Karakoram Plutonic Complex is described as a sequence of Eocene–Miocene age (Thakur, 1981). K–Ar biotite methods date the plutons at Panamik to 95.7 ± 2.1 and 96.7 ± 2.1 Ma before present (Thanh *et al.*, 2010).



Fig. 11. (a) Chumathang Hot Spring site. (b) Collecting hot spring water samples using a peristaltic pump (Photo Credits: Dr Sanjoy Som).

The hot springs at Panamik are located on a steep upward incline behind public baths and are easily accessible from the road. The active area measures $\sim 250 \text{ m} \times 100 \text{ m}$, with several sites of upwelling (mainly on the lower third). Upwelling sites are small and of low discharge. The hill was covered with grass with almost no vegetation immediately around the hot springs. Water was analysed from five sites. Site PU1 hosted green coloured biofilm, while site PU2 hosted orange-yellow biofilm with temperatures of around 62°C and a pH of 8.5. Sites PU3, 4 and 5 were hotter at around 74°C , with a pH of around 7.7 with minimal or no visible biofilm. Outflow of water was continuous and a slight smell of sulphide was present.

Chumathang springs. The Chumathang Hot Spring site (Fig. 11) (Craig *et al.*, 2013) is located along the Indus River behind an active complex of buildings. Some discharge sites closer to the complex are contaminated with outwash and seepage from the complex. The least impacted site was a cyclically geysing spring erupting every 8–9 min located by the concrete rectangular water tower ($33^\circ 21' 36.10''\text{N}$, $78^\circ 19' 26.79''\text{E}$). This site seemed the most pristine ($T = 72\text{--}8^\circ\text{C}$, $\text{pH} = 8.3\text{--}8.8$). Another site boiling more vigorously is present by the concrete wall on the river's edge, but plastic detritus littered it. The outcrops and grounds around the springs are colonized by endolithic and chiasmolithic microorganisms penetrating within the crystal grains. The Indus river completely submerges the springs during high discharge events.

Puga springs. The Puga Hot Springs (Fig. 12) are a boron-rich geothermal system (Ghosh *et al.*, 2012) located at the mouth of the Puga Valley in the north-western part of the Himalayas (Saxena and D'Amore, 1984). Boron has been proposed as a key element in the prebiotic formation of RNA, a molecule suggested as the hypothetical link between prebiotic chemistry and modern biochemistry (Orgel, 2004). Boron has been found associated with one of the oldest evidence of life, the 3.48 Ga Dresser formation in Australia (Djokic, 2015).

Like most major continental borate deposits (Grew *et al.*, 2011), the Puga system lies within a down-faulted block in an active collisional zone, with the nearby ISZ marking the boundary between the Indian and Asian continents (Craig *et al.*, 2013). Tourmaline has not been found in any hot spring deposits at Puga, and boron-bearing minerals in the system are predominantly kernite, tinalconite and borax (Ghosh *et al.*, 2012). The

hot springs occupy an area of $4 \text{ km} \times 1 \text{ km}$ and exhibit a range of geothermal activity, including geysers; mud pools; and sulphur and boratic mineral deposits.

The Puga geothermal system is fault bounded (Craig *et al.*, 2013), which restricts the geothermal activity to within the NNE–SS–trending Kyagar Tso Fault to the west and the NW–SE–trending Zildat Fault to the east, the latter representing part of the ISZ. Native sulphur and sulphate deposits along the north side of the valley suggest buried faults marking the northern boundary (Shankar *et al.*, 1976). The Puga valley is predominantly filled with alluvial cover, consisting of aeolian sand, fluvial sediments and glacial deposits encrusted with sulphur, borax and other geothermal minerals. This cover extends to depths up to 65 m, where it forms lithified breccia (Fig. 12(d)) due to mineral precipitation from the circulation of hydrothermal fluids (Singh *et al.*, 2010). Late stage magmatic activity has been suggested as the heat source for the Puga geothermal system (Chowdhury *et al.*, 1974; Saxena and D'Amore, 1984), due to high enrichments of Li, Rb and Cs in hydrothermal fluids, and results from magnetotelluric studies (Harinarayana *et al.*, 2004; Azeez and Harinarayana, 2007). Despite the main road going along the Puga river valley, accessing many of the Puga spring sites is challenging because of the swampy (and potentially hazardous) nature of the area. We identified a site (4414 m) easily accessible from the road. The site ($33^\circ 13' 39.80''\text{N}$, $78^\circ 20' 50.80''\text{E}$; Fig. 13) is an abandoned borehole. The fluid discharge site (15 cm diameter at the centre of a $\sim 1.5 \text{ m}$ diameter pool, $T = 70^\circ\text{C}$) is open and amenable to sampling and flows into four different pools of three distinct temperature (70, 40, 20°C). The pH is neutral. Hot water runoff from the springs showed the presence of coloured (pink/yellowish orange/green/grey) microbial mats (Fig. 12(e)). The release of gas bubbles was observed when the underlying sediment was disturbed, possibly from hydrogen sulphide, since there was a high abundance of sulphur cyclers observed in the area. The smell of hydrogen sulphide gas, typically released by sulphate-reducing bacteria, was also observed close to the hot springs.

Investigations and outcomes from the hot spring sites

Formation and stability of prebiotically relevant systems in hot springs. Current thinking about the emergence of early life assumes the emergence of primitive cells, which are comprised of two main components: an encapsulated genetic material



Fig. 12. (a) Puga Hot Spring crusts sample site. (b) Soluble puffy white crust in Puga Valley. (c) Differing coloration in biofilm mats at sampling sites. (d) White crust deposits in Puga Valley. (e) Algal bioherm collected from Puga Hot Springs (Photo Credits: UNSW ACA and BSIP).

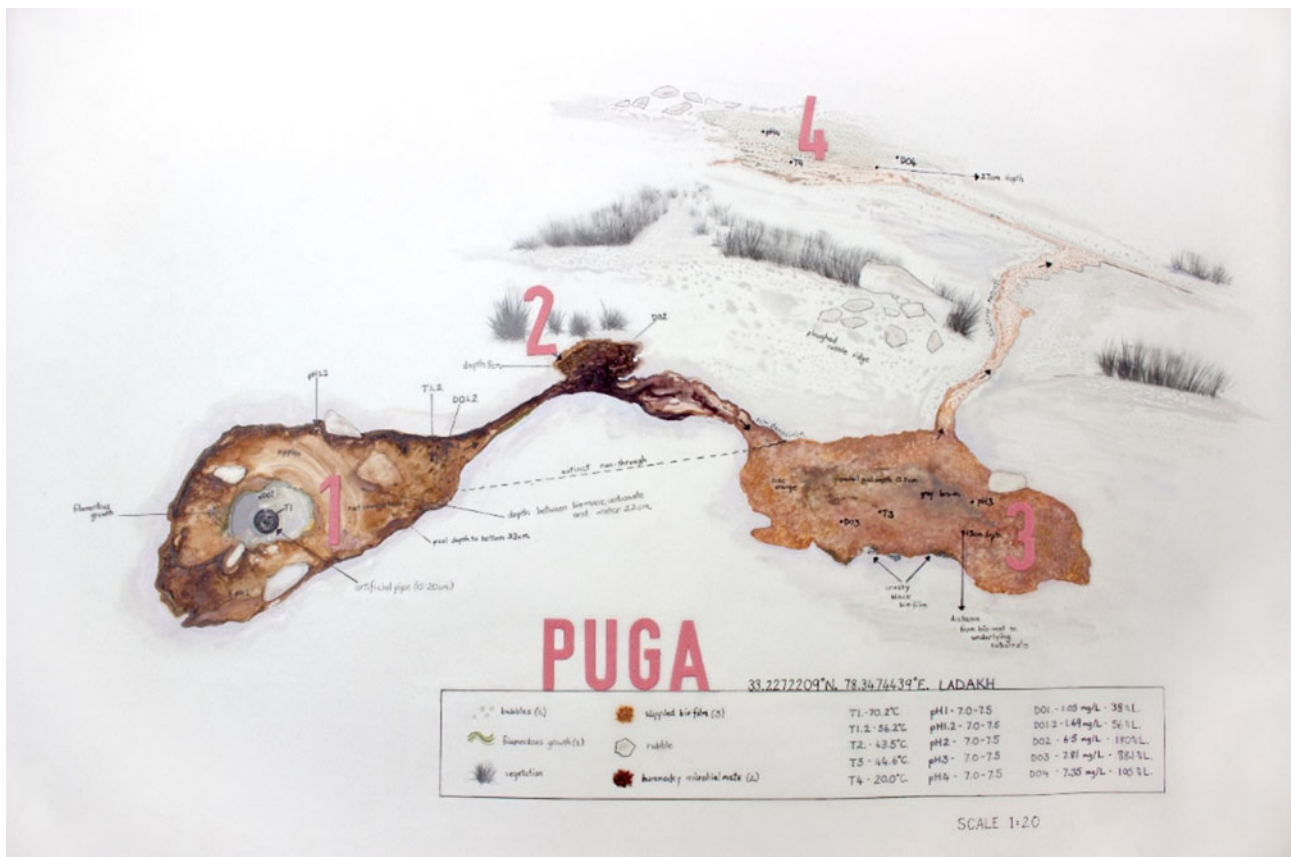


Fig. 13. Abandoned borehole discharging into four distinct pools at Puga (Art Credit: Ms Annalea Beattie).

surrounded by an encapsulating membrane boundary (Szostak *et al.*, 2001). The primitive encapsulating membranes are thought to have been composed of simple amphiphilic molecules like fatty acids (Deamer, 2017). Different fatty acids have been shown to form vesicles at specific conditions. However, the stability of such vesicles at extreme conditions of pH, temperature and variable ionic concentration is not known. We explored the stability of vesicles in Ladakh spring waters. Water samples were collected at the three different hot springs in Ladakh, namely Panamik, Chumathang and Puga. Combinations of prebiotically pertinent fatty acids and their derivatives were evaluated for the formation of vesicles and reported in Joshi *et al.* (2017). The stability of these vesicles was characterized by multiple dehydration–rehydration cycles, at elevated temperatures. Mixtures of fatty acid and glycerol derivatives were found to be the most robust, also resulting in vesicles in all the hot spring waters that were tested. Importantly, these vesicles were stable at high temperatures, and this fatty acid system retained its vesicle-forming propensity, even after multiple cycles of dehydration–rehydration. The remaining systems, however, formed vesicles only in bicine buffer. The results suggested that certain prebiotic compartments would have had a selective advantage in terrestrial geothermal niches.

Carbon metabolism in hot spring thermophiles. Hot springs having temperatures $>70^{\circ}\text{C}$ are non-conductive to photosynthesis. They are commonly inhabited by prolific biofilms of chemoheterotrophs, where researchers have had a limited understanding of how these communities derive carbon and energy, which is a requirement to maintain high levels of biomass (Schubotz *et al.*, 2015). The objective of our study was to understand the carbon metabolism in thermophiles, especially those living above 70°C . Through a ^{13}C -labelled glucose incubation experiment with thermophiles at the two thermally distinct hot springs (Pananmik and Puga), we sought to understand the light hydrocarbon consumption at different temperature and pH levels. In these experiments, slurry thermophiles from each site were transferred into the five bottles and then each bottle was closed with a butyl rubber cap followed by crimping with tin caps to make the bottles gas tight. Then, bottles were injected with ^{13}C -labelled glucose solution. These experiments were terminated at 0, 1, 2, 3, 4 h intervals. The results demonstrate high ^{13}C -labelled glucose uptake at sites with higher temperature at Puga than at those with lower temperature at Panamik site. The rate of ^{13}C -labelled glucose uptake by the microbes of Panamik Hot Spring was $3.74\text{--}96.5\text{ mmole C g}^{-1}$ of dry sediment per hour. It increased by about 2.5 times the maximum original value after 2 h. Furthermore, the ^{13}C -labelled glucose uptake in these thermophiles was compared to microbes engaging in photosynthesis and metabolic uptake at room temperature and pressure. The results (Joshi *et al.*, 2017) demonstrated a high rate of heterotrophy, allowing the maintenance of significant biomass in springs, and it was noted that the rate of heterotrophy increased with increase in temperature.

Saline lakes

Several saline lakes present in Ladakh's high-altitude, rain-shadowed region are potential analogues to lakes that existed on early Mars ($>3\text{ Ga}$), formed by evaporation of briny surface lakes (Osterloo *et al.*, 2008; Osterloo *et al.*, 2010) and/or ground-water upwelling (e.g., Glotch *et al.*, 2010). Over 600 km^2 ($\sim 25\text{ km}^2$) individual light-toned chloride deposits have been observed across the surface of Mars and appear to be associated

with the fine-scale polygonal pattern, topographic lows and fluvial channels. They are relevant to planetary geomorphologists studying early Mars and have astrobiology significance in relation to the habitability of groups studying microbial life in briny environments and salt deposits. More recently, chloride salt deposits have been observed by the MRO's High-Resolution Imaging Science Experiment (HiRISE) in the Sinus Meridiani region Opportunity rover's landing site, in relation to a lake formed ca. 3.4 billion years ago, when dry and cold conditions were already established on Mars (Hynek *et al.*, 2015). Thus, these evaporitic deposits could represent the last standing habitable water environment on the onset of dry and cold conditions on Mars (Hynek *et al.*, 2015).

Site description

Kyagar Tso. Lake Kyagar Tso is located to the south of the town of Sumdo (Fig. 14). The River Puga, together with an unnamed stream, drains into this lake (Hedrick *et al.*, 2011). Geologically, the lake is situated in the Puga gneiss complex. The lake catchment is dominated by the rocks of the Puga Formation which constitutes the lower part of the Tso Moriri crystallines. The Tso Moriri crystallines are comprised of quartzo-feldspathic gneisses, schistose bands and lenticular bodies of garnet amphibolites and eclogitic rocks. Quaternary alluvial deposits dominate the area. Lunette-shaped dunes, alluvial fans and interglacial gravel terraces surround the basin. Periglacial features including solifluction lobes and patterned ground are also present in the surrounding slopes and plains. The shoreline sediments were found to be colonized by cyanobacterial biomass, just a few millimetres below the crust.

Tso-Kar. The region is characterized by extreme climatic conditions. Temperature varies from -40°C in winter to $>30^{\circ}\text{C}$ in summer, with extreme diurnal fluctuations, i.e. <0 to $>30^{\circ}\text{C}$ (Bhattacharyya, 1989; Philip and Mazari, 2000). Mean annual precipitation (rain or snow) is $<90\text{ mm}$. Tso-Kar Lake is a fluctuating shallow (1–3 m depth) salt lake characterized by high salinity with hypersaline ($>50\%$) extremes ($\text{TDS} = 190.5\text{ g L}^{-1}$) of the Na–K– SO_4 –Cl type (Kramer *et al.*, 2014). Annual evaporation ranges from 400 to 600 mm year^{-1} (Yu *et al.*, 2001) with dense brine observed in summer when evaporation is at its maximum (evaporation exceeds precipitation). The lake is inhabited by several species of ostracods with high tolerance to salinity extremes. This lake is situated within the Taglang La Formation of the Tso Moriri Crystalline Complex, assigned as an accreted unit of the ISZ (Fig. 15). The Taglang La Formation consists of metamorphosed calcareous, marly and argillaceous metasedimentaries together with concordant bands of amphibolites (Thakur, 1992). Thick piles of Quaternary lacustrine sediments are present as a cover deposit. The basin is tectonically bounded by the Tso-Kar fault to the west (N–S) and the Tso Moriri left lateral strike-slip fault (N–S) to the east. Lake Tso-Kar receives water through a shallow overflow of lake Startsapuk Tso, another river-fed lake, situated in the same catchment. Small glacial cirques at the north-eastern and south-western side of the basin, terminal moraines along the eastern side of the basin, a lateral moraine on the western side of the basin and hummocky landscape with polished and striated clasts are the distinct glacial landforms. Fluvial activity can be observed as the terminal moraines have the fluvial erosion signatures.

Another striking feature is the raised palaeo-shorelines (highest $+98\text{ m}$ from present lake level) at the northern and southern



Fig. 14. Lake Kyagar Tso (Photo Credit: Dr Jonathan Clarke).



Fig. 15. (a) Tso-Kar Lake shoreline with abundant salt deposits (Photo Credit: Ms. Teresa Mendaza). (b) Tso-Kar salt flats (Photo Credit: Ms Anushree Shrivastava). (c) Pale pink-coloured microbial filaments on the Tso-Kar Lake shore. (d) Solifluction lobes on the hill to east side of Tso-Kar, zone of movement is 300 m wide. (e) Salt crust deposits near Tso-Kar. (f) Google Earth Image depicting rock glaciers on the north side of the valley between Puga and Tso-Kar (Photo Credits for c, d, e and f: Dr Jonathan Clarke).

sides of the basin and surrounding the lake (Fig. 16(a)). They appear as elongated terrace-like ridges of a few decimetres in height, suggesting gradual shrinkage in lake level since its formation. The hydrological evolution and climate changes of the lake are very well studied and attributed to the interplay of climate

and tectonics (Sekar *et al.*, 1994; Wünnemann *et al.*, 2008, 2010; Demske *et al.*, 2009). Thermokarst forms, frost mounds, possible 10 m high lithalsas, thermal contraction crack polygons, permafrost mounds with thick ice lenses and reticulate cryostructures are the features that demonstrate that this area undergoes

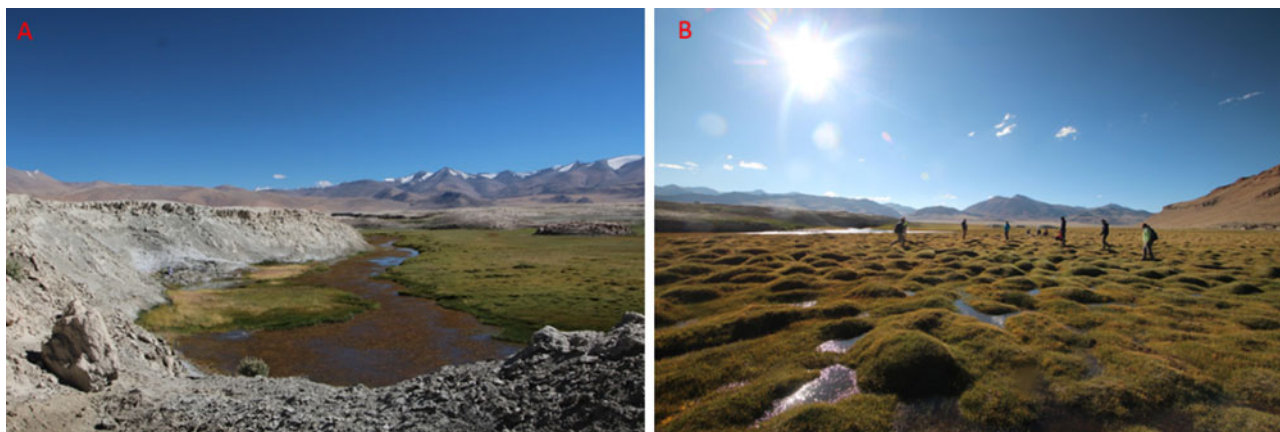


Fig. 16. (a) Raised palaeo shorelines along the northern side of Tso-Kar Lake. (b) Thermokarst frost mounds near the northern side of Tso-Kar Lake (Photo Credits: Ms Johanna Bergstörms Roos).

geomorphic changes due to permafrost activity (Fig. 16(b)). However, investigations do support the existence of discontinuous permafrost due to the presence of many small- and medium-sized ponds near the frost mounds and the larger ones in isolated thermokarst depressions (Dimri *et al.*, 1983; Bhattacharyya, 1989; Wünnemann *et al.*, 2008; 2010).

Distribution of total active biomass along the Ladakh transect

The Ladakh transect was used as an opportunity to test life detection assays in a set of diverse extreme planetary-like environments. Life detection protocols are relevant for the preparation of future life detection missions to Mars, ocean Worlds and ice-covered Moons. Brines, waters and sediment/rock samples were co-analysed using the Adenosine 5'-triphosphate (ATP) Luminometry Assay and the Lymulus Amebocyte Assay (LAL) to determine the amount of lipopolysaccharides (LPSs). Both these biomarkers are proxies for recent biological activity and active biomass distribution across the study sites (Fig. 15).

ATP Luminometry Assay

This assay detects the total ATP, which is the universal energy carrier in nature, common to all living cells. Because ATP degrades rapidly after cellular death and disruption, if detected, ATP is a proxy for total active (or recently active) biomass. The assay is based on firefly (*Photinus pyralis*) luciferase that catalyses the oxidation of D-luciferin if ATP and oxygen are present.

$$\text{ATP} + \text{d-Luciferin} + \text{O}_2 + \text{Luciferase (Mg}_2^+ \text{)} \rightarrow \text{Oxyluciferin} + \text{AMP} + \text{Pyrophosphate} + \text{CO}_2 + \text{h}\nu \text{ (560 nm)}$$

The luminometer measures the light emitted by the luciferin-luciferase enzymatic reactions binding with the ATP released by living cells. Lighting events are translated into Relative Luminosity Units (RLUs) in proportion to the amount of ATP in the sample (DeLuca and McElroy, 1978). The raw RLUs were converted into concentrations of ATP biomarker using a calibration curve and a Na₂ATP salt standard (BioControl, N. 64004-25), e.g., 1×10^{-13} moles of lyophilized adenosine triphosphate is equivalent to 37 326–42 151 RLU (N = 5). The sensitivity or limit of detection (LOD) of this assay is 1–1 000 000 fmole (1 fmole = 1×10^{-15} mole) (Hygiene comparison chart, 2006).

The ATP concentration can be further converted into total biomass based on the published values of ATP cellular equivalent. For instance, the minimum and maximum total cell abundance is calculated by assuming published values of 4×10^{-17} g ATP (Egeberg, 2000). Field protocols were applied to both liquid (water and brines) and solid samples. The analysis of sediment particles involved direct loading of 5–25 mg of homogenized material onto the swab devices. Silt to clay-sized sample particles were swabbed from the internal surface of the sterile sampling bag till the entire sample was loaded onto the swab surface. These solid samples were re-analysed in the laboratory at Birbal Sahni Institute of Palaeosciences (BSIP), Lucknow.

For the analysis of liquid samples, 100 μL aliquots were directly pipetted into the liquid sampling device. To achieve the best signal/noise ratio, dilution protocols were applied to the analysis of brines and hot spring liquid samples, which were diluted 100–1000 times in doubled distilled water (DDW) to achieve the best signal/noise ratio. Triplicate ATP analyses were performed with appropriate control standard as well as positive and negative controls to mitigate false positives and false negatives. The analysis of liquid samples was performed in the field immediately, or shortly after collection.

LAL assay

The LAL assay detects LPSs, which are primary components in the cell walls of all Gram-negative-like microbes including active, dormant or dead cells. The LAL chromogenic assay has been extensively used for quality control of pyrogens (Lipid A) in drugs. More recent, the LAL assay has been applied to bioburden monitoring in spacecraft (NASA Planetary Protection standard practices, NPR 5340, 2007), during field astrobiology trials (Eigenbrode *et al.*, 2010), and has been proposed for life detection sensors for future planetary missions. The assay has been applied in biologically low biomass rocks and minerals ($\leq 10^2$ cell equivalent g^{-1}) as well as to biomass-rich brines, sediments and soils, i.e., $\sim 10^9$ cell equivalent g^{-1} (Bonaccorsi *et al.*, 2010).

LPS samples (N = 25) were extracted under aseptic conditions; ~ 1 g of the mineral was homogenized and mixed with ~ 3.5 mL of DDW. The solution was subsequently vortexed (2 min), sonicated (10 min at 40°C) and centrifuged at high speed (6400 g) for 15 min. At the end of each extraction cycle, the LPS-enriched supernatant was transferred in a new 15 mL vial, while the

LPS-leached solid residue (pellet) underwent further extraction. This procedure was repeated three times to ensure cells' breakage, fragmentation of the LPS-bearing cells' membrane, the LPS dislodgement, its homogenization, thus to increase the analyte's concentration and maximize its detection. The final 11 mL solution was centrifuged one last time for 20 min to obtain a crystal-clear supernatant. Four 25 μL aliquots of this solution were pipetted into a laboratory-on-a chip cartridge (sensitivity range 0.5–0.005 and 1.0–0.01 EU mL^{-1}) and analysed with a Portable Test System (PTS) spectrophotometer (405–410 nm). The chip has four ports receiving the liquid sample, two for spiked and two for non-spiked sub-aliquot samples. The resulting Endotoxin Unit (EU), 1EU = 1×10^5 cell equivalent mL^{-1} of *Escherichia coli*, is translated into nanograms of LPS (ng mL^{-1}) using calibration curves built in the PTS's software. The current practical LOD for the LAL assay is 0.005 EUs, equivalent to (5×10^{-13} g of LPS) per mL of water or ca. 500 cells mL^{-1} . These protocols have been developed by co-author Bonaccorsi during previous field expeditions to extreme environments (Bonaccorsi and Stoker, 2008; Bonaccorsi *et al.*, 2010).

Results and discussions

The LAL and ATP assays were successfully used in the field to determine the distribution of living biomass across the Leh-Ladakh system. Results are summarized in Fig. 17. Overall, 25 samples were assayed for LAL, while 29 were assayed for ATP. Only 16 samples out of a pool of 38 were co-analysed for both biomarkers. As showed in Fig. 17B, ATP correlates well with the LPS amount within each study environment for Hunder System, hypersaline lakes and shorelines, Tso-Kar Permafrost and hot springs ($R^2 = 0.5-1$). However, there is no significant correlation between ATP and LPS ($R^2 = 0.045$, $N = 16$) when considering the whole dataset. Furthermore, the variation of ATP and LPS biomarkers can be different such as across five different inter-dune ponds in Hunder; specifically, the ATP concentration was extremely variable (211 ± 202 fmol mL^{-1} ; $N = 5$) in contrast to the fairly constant LPS content in randomly sampled ponds (2.52 ± 0.09 ng mL^{-1} ; $N = 3$).

Overall, across the Ladakh transect, the LAL assay yielded values of lipid biomarker (LPSs) between 2.5 and $\sim 5 \times 10^3$ ng mL^{-1} in water and brines and $\sim 16-1.1 \times 10^5$ ng of LPSs per gram (ng g^{-1}) in sediments and rocks. More specifically, the distribution of ATP biomarkers is mostly like the LPS one. The highest concentrations were measured in briny and clay-rich environments in the Tso-Kar region, particularly the brines from Tso-Kar Lake (10^4 fmol mL^{-1} ATP and 4.9×10^5 ng mL^{-1} LPSs), its cyanobacteria-rich sand-to-gravel supported shorelines ($\sim 5.0 \times 10^5$ fmol g^{-1} ATP and 1.11×10^5 ng g^{-1} LPS) and the clay-rich permafrost (10^4 fmol g^{-1} ATP and 4.33×10^5 ng g^{-1} LPS). The lowest concentration of total ATP was detected in a few hot spring water (test bed samples) and freshwater pond/stream environments ($0.0-6.0 - 11$ fmol mL^{-1} ATP and $2-3$ ng mL^{-1} LPS) (Fig. 17(a)).

The lowest concentrations of measurable LPSs were found in the water samples from hot springs and freshwater ponds/stream environments; the highest concentrations were measured in the brines of the Tso-Kar Lake (i.e. 490×10^3 ng mL^{-1}), the cyanobacteria-colonized shoreline (ca. 111×10^3 ng g^{-1} LPS) and the permafrost-associated ice-mud grains mix, particularly in the clay-supported rounded particles embedded in the permafrost's ice lenses (i.e. 433×10^3 ng g^{-1} LPS).

Glacial high passes

To explore the parametric biological content of the most extreme high elevation desert, representative aliquots of composite samples were assayed from two contrasting surface settings (0–2 cm-depth) on the North-facing slope at Taglang La. The first sampled site, a moss-free, dark-toned quartz-rich micaceous regolith from solifluction lobes (Fig. 5(b)) contained a 2.5-fold more lipid biomarker (39 ng g^{-1} LPS) than the carbonaceous (limestone) material (ca. 16 ng g^{-1} , LPS) atop the light-toned vegetation-barren outcrops (Fig. 5(b)). It is unknown whether this difference is significant or related to actual environmental differences (nearby moss-colonized patches, higher ground moisture, different regolith's composition) rather than the non-systematic sampling effort (just one sample from each lithology was analysed). In any case, the hyper-arid contrasting soil types from Taglang La contain 39 ng of lipid biomarker per gram (ng g^{-1}). The two different contrasting bedrock lithologies from Taglang La may contain a different living microbial ecology to be tested in future studies. In both cases, the low biomass measured was consistent with the aridity/(hyper-aridity?) observed at this location, i.e., vegetation-barren, mechanically weathered regolith with estimated top soil water content $<2-5\%$, RH, air $<5-10\%$ associated. Interestingly, Taglang La's rocky desert might contain biomass levels comparable to those in oligotrophic deserts worldwide (Antarctic Dry Valleys, Atacama and the Mojave Desert). Specifically, similar levels of LPS were found by Bonaccorsi *et al.* (2010) using similar LAL protocols: $\sim 0.4-2.4$ ng g^{-1} in arid and hyper-arid core of the Atacama Desert (precipitation $\sim 2-11$ mm year $^{-1}$) and $\sim 44-140$ ng g^{-1} in volcanically-derived soil from the arid Death Valley (precipitation: $\sim 40-250$ mm year $^{-1}$).

Hunder dunes and ephemeral ponds

The distribution of LPS and ATP biomarker was evaluated across several subsystem environments within the Hunder dune field. A total of 14 different samples (Fig. 17) were taken from dry sand dunes' crest and bottom (HU-Pond_sand, $N = 3$), inter-dune ponds (HU-Pond_W, $N = 7$), pond's underwater sediments ($N = 1$), wind eroded, dry mud-cracked horizons, soaked mud from the pond's shoreline ($N = 2$). The ATP biomarker across the six investigated ponds was quite variable ($30-531$ fmol mL^{-1}), plausibly in relationship with the fluctuating level of active biomass present in the ephemeral water (i.e., clear water versus organic debris-rich water); in contrast, the Lipid A content resulted fairly constant across three different ponds (Fig. 17A). The lowest content of ATP biomass measured in pond samples was comparable to 32 fmol mL^{-1} ATP measured in the single sample from the Skyok River (HU_river_w) across the dune field. When considering the LPS variability across and individual pond system, Hunder dune's short-lived fresh water in pools contains ca. 2.5 ng of lipid biomarker per millilitre (ng mL^{-1}) with LPS biomarkers concentrated in the underwater sediments (17 ng g^{-1} LPS and 823 fmol g^{-1} ATP). The surrounding clay beds preserve 1000 times more biomarkers (lipid biomarker concentrations of $9-165 \times 10^3$ ng g^{-1} LPS and 1329 fmol g^{-1} ATP) than the encasing sand dunes ($\sim 19-112$ fmol g^{-1} ATP and $\sim 4-8$ ng g^{-1} LPS) ($4.18.2$ ng g^{-1}) given the propensity for clay to preserve organics. On Earth as well as on Mars, the reactivity between regolith's minerals and organics affects preservation and detection of organic matter and the direct evidence of life (e.g., Klein *et al.*, 1976; Navarro-González *et al.*, 2010). Organics are poorly preserved in oxidising environments (Bonaccorsi *et al.*, 2010; Davila *et al.*, 2011), as well as porous

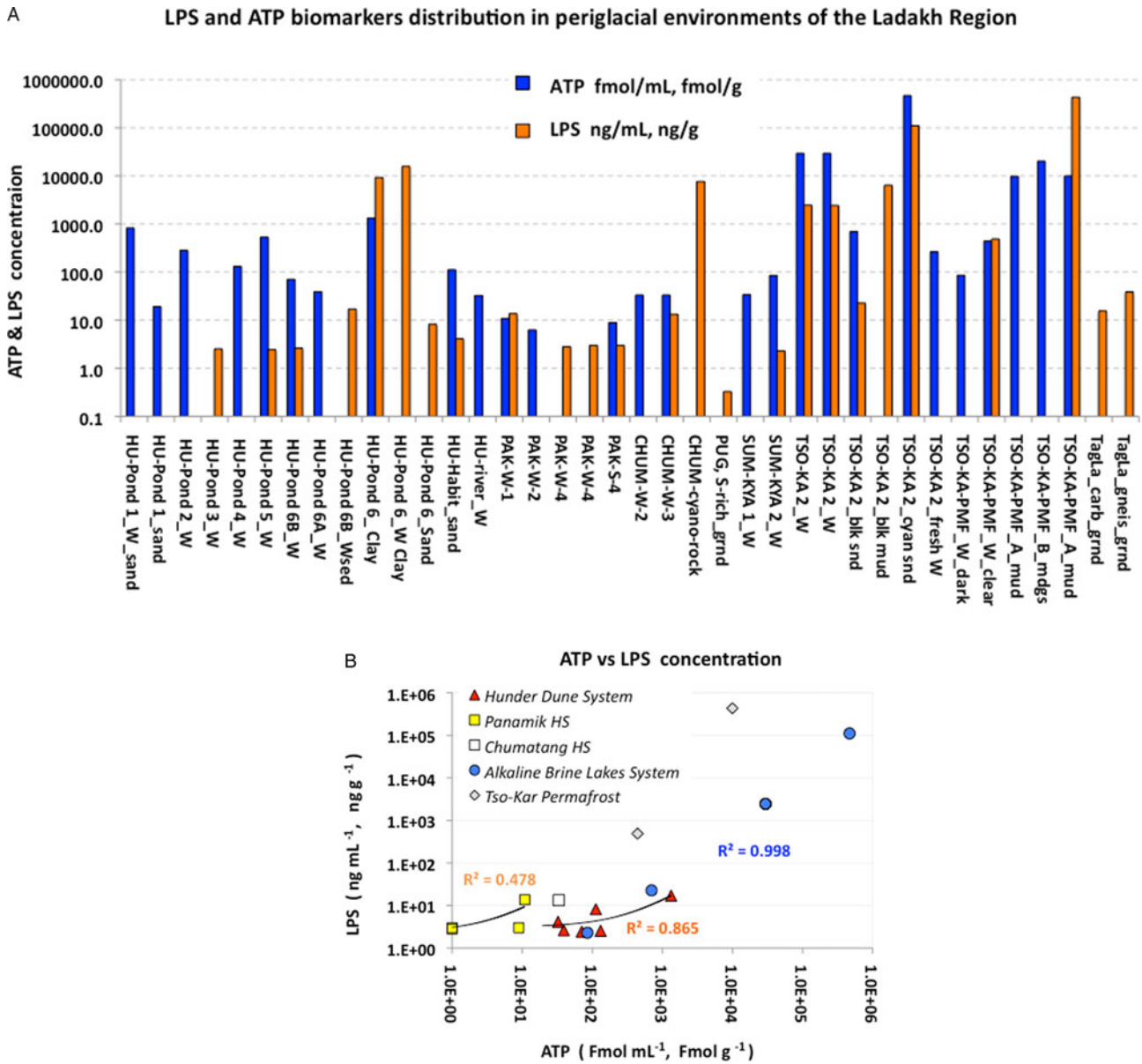


Fig. 17. (a) Concentration distribution of LPS and ATP biomarkers in collected samples. (b) Plot showing positive correlations between LPS and ATP biomarker pools for each assessed environment. Only 17 samples co-analysed for both biomarkers – out of the total dataset (Fig. 17(a)) – are plotted.

and coarser-grained materials (sands, gravels, sandstones), but they are in clay-rich deposits against oxidation (e.g., Hedges and Keil, 1995; Bonaccorsi and Stoker, 2008). Dissolved organics adsorbed on mineral surfaces (D’Acqui *et al.*, 1998; Kleber *et al.*, 2005; Kaplan *et al.*, 2014) can be preserved against microbial decay (e.g. Mayer 1994; Bock and Mayer, 2000; Aggarwal *et al.*, 2006; Yu *et al.*, 2009). Clay-bearing deposits, including the mid Hesperian Sheepbed unit (Thomson *et al.*, 2011; Grotzinger *et al.*, 2014), have been targeted by the NASA Mars Science Laboratory Curiosity mission in Gale Crater for sampling, because of their expected high habitability potential (related to liquid water) and preservation of organics (e.g., Farmer and DesMarais 1999; Grotzinger *et al.*, 2014). It is thought that Sheepbed clay deposits would have formed in relatively pH-neutral surface freshwater during a period of increasing aridity, yet characterized by episodic rainfall (Barnhart *et al.*, 2009; Andrews-Hanna and Lewis, 2011). The role of multiple short-

lived wetting events in the formation of sedimentary clay minerals is not well understood (e.g. Milliken and Bish, 2010; Ehlmann *et al.*, 2013), but we know that terrestrial smectite clays can only form under dry, i.e., mean annual precipitation <50 cm year⁻¹, and circum-neutral/alkaline, i.e., pH 6.5–7.8, conditions (Schiffman *et al.*, 2000).

Hot springs

Because of high temperatures and the presence of geothermal minerals (e.g., Singh *et al.*, 2010) *in situ* life detection in hot springs environment can be very challenging and at the possible lowest end of the detection limit of any life detection instrumentation. Therefore, a few water, sediments and rock samples were analysed in order to develop protocols suitable for life detection of ultra-low biomass (oligotrophic) in hydrothermal mineral-rich environments, and water chemistries potentially interfering with the wet chemistry of the biological assays (low signal-to-noise

ratio). The sample suite consisted of four water samples and one sediment sample from Panamik (PAK-W 1, 2 and 4; PAK-S-4); one water sample (CHUM-W-2) and a composite rock sample (CHUM-cyano-rock) gathered from outcrops nearby Chumatang Hot Springs; and a desiccated mineral deposit sample from the Puga compound (PUG-S-rich_grnd). The concentration of total ATP in four water samples from Panamik ranged from ca. 6.0 to 11 fmoles mL⁻¹ in samples PAK-W-1 and PAK-W-2, respectively, with the exception of water taken from the hottest spot Site 4 (PAK-W-4, N=5), which yielded non-measurable ATP lipid (below LOD <0.2 fmoles mL⁻¹). The same water sample, however, contained low but measurable LPS (2.90 ± 0.13 ng mL⁻¹; N=4), yet, one of the lowest concentrations detected across the entire transect. The above results, as well as other measurements from several sets of geological samples, demonstrate that the LAL assay can provide a reproducible estimate of LPS-based biomass in complex environmental materials. Interestingly, the associated sediment slur (PAK-S-4, N=5) contained 2.5 ng g⁻¹ LPS and 9.0 fmoles g⁻¹ of total ATP, suggesting that living biomass (or residual ATP biomarker) is better concentrated/preserved in the muddy slur. This result is consistent with the lowest rate of 13C-labelled glucose uptake by the microbes of Panamik Hot Spring (3.74 mmole C g⁻¹ of dry sediment per hour) (~74°C, pH = 7.7) co-analysed for ATP.

By comparison, the water sample from Chumatang yielded higher amounts of LPSs (13 ng mL⁻¹) and ATP (33.2 fmoles mL⁻¹) than Panamik's and displayed the same range of biomass of the freshwater sample from the Shyok River (~33.4 fmoles mL⁻¹) in the Hunder region. The LPS content of outcrops and gravelly supported grounds around Chumatang Hot Spring was also high e.g. 7650 ng g⁻¹, in relation to endolithic and chiasmolithic microorganisms colonising within the minerals' grains.

We did not attempt to perform systematic measurements of the biomarker distribution in the Puga Hot Spring, which is beyond the scope of this work; rather, we analysed sulphur-laden dirt as a test bed for possible life detection in relevant sulphur-rich planetary surfaces. This sulphur-rich ground sample (dry) yielded the lowest amount of measurable LPS (0.38 ng g⁻¹). The attempted measurement was extremely challenging as it yielded several false negatives (N=6), plausibly due to a combination of ultra-low biomass, originally present in the dry dirt, and sulphur chemistry interfering with the LAL assay.

Alkaline brine lakes

To preliminarily assess the total biomass amount distribution at the Tso-Kar Lake, we analysed six samples across a traverse from hyper saline-dominated to fresh water-dominated environments. The former, proximal to the shoreline, comprised brines, greenish-grey sand and dark grey mud at the interface with, or beneath the evaporitic crust (Fig. 15(b) and (e)). The latter, 200–300 m away from the shoreline, consisted of cyanobacteria-colonized glacial debris and glacial melt water-sourced ponds nestled in a field of moss-colonized bogs/peats. The biomarker concentration of Tso-Kar brines (2.5 × 10³ ng mL⁻¹ LPS; 3 × 10⁴ fmoles mL⁻¹ ATP) resulted three to four orders magnitude higher than that of water samples (N=2) from the Kyagar Tso/Sumbdo Lake, i.e. ~2 ng mL⁻¹ LPS; 35–80 fmoles mL⁻¹ ATP (Fig. 17(a)). It is unclear whether or not the remarkable difference in biomarker content between the samples from the two lakes reflects the opportunistic sampling (not a significant set of samples to draft any conclusion) rather than (i) a higher preservation of ATP and LPS biomarker in brines versus salty water, (ii) an

actual presence of living biomass or (iii) a combination of both. Interestingly, the LPS content of clays versus non-clay materials beneath the evaporitic deposits, sandy to silty-clay shoreline sediments ranges from ~23 ng g⁻¹ (sand) to 6400 ng g⁻¹ (mud), consistently with the preferential preservation of organics in clays. Further away from the shoreline, melt water (freshwater) flushed sediment contains the highest amount of biomarkers of the entire transect (~5.0 × 10⁵ fmoles g⁻¹ ATP; ~10⁵ ng g⁻¹ LPS), plausibly in relation to the cryptic, but widely distributed thin layer of living cyanobacterial biomass hiding just a few millimetres below the periglacial debris. Comparatively, the cyanobacteria-colonized distal sands contained a three-order magnitude higher ATP (467 261 fmoles g⁻¹, ca. 4.7 × 10⁵) than the proximal shoreline sand (~700 fmoles g⁻¹ ATP, or 7.0 × 10²), or the freshwater ponds in the bogs around the lake (264 or 2.6 × 10² fmoles mL⁻¹ ATP).

Wet chemistry-based life detection assay of complex evaporite systems – including briny extreme salinity environments (TDS = 190.5 g L⁻¹) (Kramer *et al.*, 2014), produced quite challenging results. First, hyper-saline environments can be poorly conducive to microbial life (refs. here), therefore, hosting low to very low levels of biomass (Fig. 15) requiring detection assays with high sensitivity (i.e., ultra low LOD). Second, independently by the specific content of microbial life in brines, life detection in evaporitic environments is jeopardized by possible chemo-physical interferences between the salts and the aqueous chemistry of the bioassays in question. The latter issue produced particularly relevant results during our first attempt to analyse evaporites containing obvious life, such as the pink coloured microbial filaments on the shoreline of Tso-Kar Lake (Fig. 14). Non-diluted Na–K–SO₄–Cl dense brine samples from this environment yielded no biomarkers (false negatives), but the highest biomass was instead detected as soon as the same sample was diluted 100–1000 times with distilled water (Fig. 15(a)–(e)). The Tso-Kar Lake could represent a big sink system of organic matter and living biomass from distal regions around the basin and supported by glacier meltwater (source). This can be explained by the source to sink processes of cyanobacteria-associated biomarker. The Tso-Kar Lake ecosystem displayed very high levels of cyanobacterial biomass possibly supported by glacier meltwater. The habitability potential is enhanced by this source of freshwater flushing amounts of loose cyanobacterial biomass from the colonized shorelines into the Tso-Kar Lake basin. It is possible that the high level of total biomass we found in the lake brines – and the associated lacustrine mud – represents the sink of the freshwater-supported living biomass flushed into the lake by glacier meltwater. At this stage, it is not possible to determine whether the total ATP measured in the lake is ATP biomarker (extracellular free ATP) preserved in salts and clays, rather than microbial ATP from intact and/or living cells and spores (microbial ATP). Further investigation is warranted to address the distribution of living biomass in the brine ecosystem. Saline lakes existed on ancient Mars and their palaeo deposits may still preserve lipid biomarkers as signatures for ancient life.

Tso-Kar permafrost region

The permafrost mound along the Tso-Kar palaeo-shoreline included cryo structures such as clear lenses of ice, in a matrix of dark grey icy mud matted with patches of yellowish silt-clay-ice frozen mix. In each matrix, grey and yellowish frozen mud and ice lenses were sampled at dm to sub-cm scale and contained biomarkers concentrations ranging from 10³ to 10⁴ magnitude, respectively, i.e., 4.9 × 10²–4.33 × 10⁵ ng g⁻¹ LPSs (N=2), and

8.6– $\sim 2 \times 10^4$ fmol mL⁻¹ ATP ($N = 5$). Specifically, the dark-grey muddy melt (Site 1B) contained five times lower amount of total ATP (85.6 fmol mL⁻¹), compared to the clear ice melt water (441 fmol mL⁻¹ ATP) from the dark grey permafrost matrix (Site 1D). The other material embedded in the permafrost matrix ($N = 3$) were yellowish mud grains with very high concentrations of ATP ($\sim 1 \times 10^4$ – 2×10^4 fmol g⁻¹, $N = 3$) and LPS (433 350 ng g⁻¹), which represent the highest amount measured across the whole transect (Fig. 17(b)). The analysis of two sub aliquots from the same subsample (TSO-KA-PMF_A_mud) yielded reproducible values (9820 and 9970 fmol g⁻¹), while the assay of another whole individual grain yielded a twofold amount of ATP (20 260 fmol g⁻¹). These mud particles differed from the embedding dark grey permafrost matrix by colour (yellowish), texture – high cohesive, retained after the permafrost melted up, and high content of living biomass, or preserved biomarkers. These mud particles resulted very similar to sub-cm semi-rounded particles, referred as at to Mud Grains, or MDGS founded ice-bounded and/or glaciogenic sediments and glacial-marine sediments scoured by glaciers/ice streams from the Antarctic subglacial interiors (e.g., Kluiving *et al.*, 1999; Bonaccorsi *et al.*, 2000; 2005, and refs. therein). Mud-supported particles were identified in the Ross Ice Shelf (RIS) sea-ice and sediment cores (Webb *et al.*, 1979; Zotikov and Jacobs, 1985), ice cores from Antarctica and Greenland (Gow and Meese, 1996) and Lake Vostok ice core's basal sediments (Jouzel *et al.*, 1999) as well. Overall, their unique features point to 'freeze in' processes aiding the concentration of organic biomarkers closely coupled to ice stream erosional/depositional processes occurring at the ice-sheet/sediment interfaces (Bonaccorsi *et al.*, 2005), which could be also the case for the Tso-Kar cryostructures. Detecting biomarkers in ice-bound clays in permafrost's reticulate cryostructures, or other ice-bound environments, offers a significant opportunity to train for life detection missions to the polar and mid-latitude regions of Mars, or to the ice sheet-dominated surface regions on Ocean Worlds, where similar biomarker-concentrating ice-non-ice mix fine-grained materials could be accessed for sampling. Non polar ice deposits are present at mid-latitudes on Mars and appear more widespread and common than previously believed.

Education and public engagement

This expedition was a follow-up of the Spaceward Bound expedition series (initiated at the NASA Ames Research Center in 2006) regularly held within the USA and other countries with a special focus on education outreach and fieldwork training of participating international and local educators and students (e.g. Bonaccorsi *et al.*, 2017). The expedition facilitated collaboration between Indian and international research groups in the field and in the laboratory. As a key element of this expedition, the participants engaged in initial discussions towards the formation of an astrobiology research roadmap for India. Towards this, the team members engaged in end-of-day discussions conducted hands-on science projects with Ladakhi students from nomadic village primary schools, and interacted with undergraduate science and engineering students in New Delhi, at the end of the expedition.

Conclusions

The 2016 multidisciplinary expedition to explore Ladakh was fundamental in assessing the astrobiological potential of the

visited sites. Several site-specific experiments were conducted, both during and after the expedition which added to our understanding of the region. The main outcomes of the expedition are listed below:

- The high passes of Ladakh, Khardung La and Taglang La are unique analogues for early Mars with their combination of low atmospheric pressure, high UV radiated soils, permafrost and active periglacial activity, glaciers and glacier melt water pools. The environment in Khardung La supported deliquescent melting of calcium chloride salts based on tests conducted with the HABIT instrument prototype, designed for the ExoMars 2020 mission. The cold, desert environment of these passes also provided an ideal setting to develop and implement regolith-landform mapping methodology for these terrains.
- The Hunder region with its valley dunes and ephemeral pools provides an early Mars-like (Noachian or later) setting, an ideal environment for preservation of microorganisms. Rose diagrams generated using QGIS software indicated an unusual trend of seasonal dependency on dune orientation and wind direction due to wind changes being within 60° and mild weather variation due to the region. Such a technique could prove useful in understanding wind-surface interactions for regions on Mars or Earth where local weather information is not available.
- Ladakh hot springs of Panamik and Puga showed higher heterotrophy rates with significant biomass for higher discharge temperatures. The water samples also showed robust combinations of pertinent prebiotic mixtures that were stable at high temperatures and retained their functionality after multiple cycles of dehydration-rehydration.
- The saline lake shoreline sediments of Kyagar Tso and Tso-Kar were colonized by cyanobacteria just a few millimetres below the crust. The Tso-Kar Lake could represent a big sink system of organic matter and living biomass from distal cyanobacteria-colonized around the basin sustained by glacier meltwater (source).
- Permafrost activity, a unique phenomenon seen on Mars and rarely found on Earth was observed in the area. Tso-Kar permafrost 'granulated' cryo structures contained an unusually high amount of biomass. 'Freeze in' processes at the ice-sediment interface might be responsible for the concentration and storage of organic biomarkers in glacial sediments of planetary environments; thus suggesting glaciated areas as a primary target for life detection.
- Life detection assay methodology (ATP and LAL assays) was tested across the entire Ladakh transect, but the analysis of hypersaline extremes and clay-rich environments was affected by false negatives, jeopardising scientific discovery. Analytical protocols tested during the expeditions, also including dilution, resulted critical to the correct evaluation of biomass content in these planetary-like geological environments.
- This analysis method is relevant to several future off-Earth missions to worlds (Mars, Ocean Worlds and Icy Moons) that could potentially harbour life.
- The co-analysis of ATP and LPS biomarkers provided the first known measurement of total active biomass in the region. Tso-Kar evaporites and permafrost ice-bound clays contained the highest biomass, hot spring water samples, sand dunes and surface regolith from Tang La glacial high pass, the lowest. The clay beds associated with the inter-dune ponds showed

1000 times higher LPS amounts than the surrounding sands, given the propensity for clays to preserve organics.

- In regions of cold arid environments, HABIT discovered the existence of the interaction of the diurnal water cycle with salts. These can serve as liquid water reservoirs and be comparable to areas where ice is melting. This was confirmed by life detection assays finding the highest amount of LPS-based biomass in the brines of the Tso-Kar Lake ($\sim 5 \times 10^5$ ng mL⁻¹) and in the clay-supported permafrost (i.e. $\sim 4 \times 10^5$ ng g⁻¹ LPS). Finally, the clay beds around the dune ponds showed 1000 times higher LPS amounts compared to adjacent sands.
- This campaign has confirmed the relevance of clays, brines and permafrost as interest targets of research on Mars for life detection and biomarker preservation as a proxy for recent and ancient life.
- Last but not least, as follow-up of the Spaceward Bound expedition series, the Ladakh Spaceward Bound expedition promoted collaboration between the US, Indian and international research groups; engaged local schools and communities in the exploration of the space and Mars; and sat up the stage for an astrobiology research roadmap for India.

Author ORCID.  Siddharth Pandey, 0000-0002-4123-3949

Acknowledgements. The team would like to express its gratitude to Birbal Sahni Institute of Palaeosciences, Department of Science and Technology, Office of Chief Wildlife Warden of Ladakh, Government of India for helping arrange the requisite clearances and permits for the conducted work. Project mentoring and guidance provided by Spaceward Bound members at NASA Ames Research Center. Financial and logistics support provided by Tata Motors Ltd, Inspired Journeys Co, Pearl Travels Ltd and National Geographic Traveller India. Website and IT support provided by the Blue Marble Space Institute of Science. Audio-video documentation support provided by Astroproject India and The Highroad Co.

References

- Aggarwal V, Li H and Brian J** (2006) Triazine adsorption by saponite and beidellite clay minerals. *Environmental Toxicology and Chemistry* **25**, 392–399.
- Andrews-Hanna JC and Lewis KW** (2011) Early Mars hydrology: 2. Hydrological evolution in the Noachian and Hesperian epochs. *Journal of Geophysical Research* **11**, 1–20.
- Azeez KA and Harinarayana T** (2007) Magnetotelluric evidence of potential geothermal resource in Puga, Ladakh, NW Himalaya. *Current Science-Bangalore* **93**, 323.
- Barnhart CJ, Howard AD and Moore JM** (2009) Long-term precipitation and late-stage valley network formation: landform simulations of Parana Basin, Mars. *Journal of Geophysical Research* **114**, E01003.
- Bhattacharyya A** (1989) Vegetation and climate during the last 30,000 years in Ladakh. *Paleogeography, Paleoclimatology, Paleoecology* **73**, 25–38.
- Bock MJ and Mayer L** (2000) Mesodensity organo-clay associations in a near-shore sediment. *Marine Geology* **163**, 65–75.
- Bonaccorsi R and Stoker CR** (2008) Science results from a Mars drilling simulation (Rio Tinto, Spain) and ground truth for remote observations. *Astrobiology* **8**, 967–985.
- Bonaccorsi R, Burckle L, Brambati A, Piotrowski MA, Quaia T, Finocchiaro F and Piani R** (2000) Multi-component analyses on Diamicton Mud Grains (GC Basin, Ross Sea, Antarctica). Suppl. to EOS, May 9, 2000. P. 269.
- Bonaccorsi R, Burckle L, Brambati A and Piotrowski MA** (2005) Constraining subglacial settings using clay-supported IRD (Mud grains) in Antarctic marine sediment: a framework for astrobiology. In Hoover R (ed.), *NATO ASI Perspectives in Astrobiology*. Amsterdam, The Netherlands: IOS Press, pp. 221–232.
- Bonaccorsi R, McKay CP and Chen B** (2010) Biomass and habitability potential of clay minerals and iron-rich environments: testing novel analogs for Mars Science Laboratory landing sites candidates. *Philosophical Magazine* **90**, 2309.
- Bonaccorsi R, McKay CP, Mogul R, Boston P, Willson D, Heldmann J, Baker L, Cowan D, Pandey S, Sharma M, Sun H, Blank JG, Stoker CR, Mogosanu IH, Campbell KA, Phartiyal B, Rask JC and Clarke J and the 2006–2016 SB Teams** (2017) Spaceward Bound's 11-year History: To extreme environments on Earth and Beyond. [Paper #3289]. Astrobiology Science Conference, April 24–28, 2017. Mesa, Arizona (LPI Contrib. No. 1965).
- Chowdhury AN, Handa BK and Das AK** (1974) High lithium, rubidium and caesium contents of thermal spring water, spring sediments and borax deposits in Puga valley, Kashmir, India. *Geochemical Journal* **8**, 61–65.
- Clarke JDA and Pain CF** (2004) From Utah to Mars: regolith-landform mapping and its application. In Cockell CS (ed.), *Mars Expedition Planning*. American Astronautical Society Science and Technology Series, **107**. Springfield, VA: American Astronautical Society, pp. 131–160.
- Cockell CS, Catling DC, Davis WL, Snook K, Kepner RL, Lee P and McKay CP** (2000) The ultraviolet environment of Mars: biological implications past, present, and future. *Icarus* **146**, 343–359. DOI: 10.1006/icar.2000.6393.
- Craig J, Absar A, Bhat G, Cadel G, Hafiz M, Hakhoo N, Kashkari R, Moore J, Ricchiuto TE, Thurow J and Thusu B** (2013) Hot springs and the geothermal energy potential of Jammu Kashmir State, NW Himalaya, India. *Earth-Science Reviews* **126**, 156–177.
- D'Acqui LP, Daniele E, Fornasier F, Radaelli L and Ristorri GG** (1998) Interaction between clay microstructure, decomposition of plant residues and humification. *European Journal of Soil Science* **49**, 579–587.
- Davila AF, Gross C, Marzo GA, Fairén AG, Kneissl T, McKay CP and Dohm JM** (2011) A large sedimentary basin in the Terra Sirenum region of the southern highlands. *Icarus* **212**, 579–589. DOI: 10.1016/j.icarus.2010.12.023.
- Deamer D** (2017) *The Role of Lipid Membranes in Life's Origin*. Life (Basel, Switzerland), **7**, doi: 10.3390/life7010005.
- Deluca M and McElroy WD** (1978) Purification and properties of firefly luciferase. *Methods in Enzymology* **57**, 3–15.
- Demske D, Tarasov PE, Wünnemann B and Riedel F** (2009) Late glacial and Holocene vegetation, Indian monsoon and westerly circulation dynamics in the Trans-Himalaya recorded in the pollen profile from high-altitude Tso Kar Lake, Ladakh, NW India. *Paleogeography, Paleoclimatology, Paleoecology* **279**, 172–185.
- Dimri DB, Baranwal M and Biswas UK** (1983) Integrated geophysical studies in Tso Kar Basin, District Ladakh. & K., India. *Indian Minerals* **37**, 39–46.
- Djokic T** (2015) Assessing the link between Earth's earliest convincing evidence of life and hydrothermal fluids: The c. 3.5 Ga Dresser Formation of the North Pole Dome, Pilbara Craton, Western Australia. Unpublished M.Phil. thesis, University of New South Wales Australia, 160p.
- Dortch JM, Owen LA and Caffee MW** (2010) Quaternary glaciations in the Nubra and Shyok valley confluence, northernmost Ladakh, India. *Quaternary Research* **74**, 132–144.
- Dvorkina AY and Steinberger EH** (1999) Modeling the altitude effect on solar UV radiation. *Solar Energy* **65**, 181–187.
- Egeberg PK** (2000) Porosity, particle diameter, ATP content and carbon and nitrogen composition of ODP Site 164-994 sediments. PANGAEA. <https://doi.org/10.1594/PANGAEA.804535>.
- Ehlmann BL, Berger G, Mangold N, Michalski JR, Catling DC, Ruff SW, Chassefière E, Niles PB, Chevrier V and Poulet F** (2013) Geochemical consequences of widespread clay mineral formation in Mars' ancient crust. *Space Science Reviews* **174**, 329–364.
- Eigenbrode J, Benning L, Tobler D, Rodriguez-Blanco J, Fogel M, Amundsen HEF, Callahan M, Dworkin J, Glamoclija M, Glavin D, Kerr L, Kish A, Mahaffy P, McAdam A, Steele A and Voytek M** (2010) Organic Biosignatures and Habitat Features of Near-Surface Glacial Ice in Svalbard. Astrobiology Science Conference 2010: Evolution and Life: Surviving Catastrophes and Extremes on Earth and Beyond. 1538. 5546.
- Eisenberg L** (2003) Giant stromatolites and a supersurface in the Navajo Sandstone, Capitol Reef National Park, Utah. *Geology* **31**, 111–114.

- Farmer J and DesMarais DJ** (1999) Exploring for a record of ancient Martian life. *Journal of Geophysical Research-Planets* **104**, 26,977–26,995.
- Fuchs G and Linner M** (1995) Geological Traverse across the Western Himalaya – a Contribution to the Geology of Eastern Ladakh, Lahul, and Chamba. *Jb. Geol. B.-A* ISSN 0016–7800 655–685.
- Ghosh W, Mallick S, Haldar PK, Pal B, Maikap SC and Gupta SKD** (2012) Molecular and cellular fossils of a Mat-like microbial community in geothermal boratic sinters. *Geomicrobiology Journal* **29**, 879–885.
- Glotch TD, Bandfield JL, Tornabene LL, Jensen HB and Seelos FP** (2010) Distribution and formation of chlorides and phyllosilicates in Terra Sirenum, Mars. *Geophysical Research Letters* **37**, L16202. DOI: 10.1029/2010GL044557.
- Gow AJ and Meese DA** (1996) Nature of basal debris in the GISP2 and Byrd ice cores and its relevance to bed processes. *Annals of Glaciology* **22**, 134–140.
- Grew ES, Bada JL and Hazen RM** (2011) Borate minerals and origin of the RNA world. *Origins of Life and Evolution of Biospheres* **41**, 307–316.
- Grotzinger JP, Sumner DY and Kah LC** (2014) A habitable fluvio-lacustrine environment at Yellowknife Bay, Gale crater. *Mars Science* **343**, 124277.
- Hamilton VE, Morris RV, Gruener JE and Mertzman SA** (2008) Visible, near-infrared, and middle infrared spectroscopy of altered basaltic tephra: spectral signatures of phyllosilicates, sulfates, and other aqueous alteration products with application to the mineralogy of the Columbia Hills of Gusev Crater, Mars. *Journal of Geophysical Research* **113**, E12S43.
- Harinarayana T, Azeez KA, Naganjaneyulu K, Manoj C, Veeraswamy K, Murthy DN and Rao SPE** (2004) Magnetotelluric studies in Puga valley geothermal field, NW Himalaya, Jammu and Kashmir, India. *Journal of Volcanology and Geothermal Research* **138**, 405–424.
- Hedges JI and Keil RG** (1995) Sedimentary organic matter preservation: an assessment and speculative synthesis. *Marine Chemistry* **49**, 81–115.
- Hedrick KA, Seong YB, Owen LA, Caffee MW and Dietsch C** (2011) Towards defining the transition in style and timing of quaternary glaciation between the monsoon-influenced greater Himalaya and the semi-arid Transhimalaya of Northern India. *Quaternary International* **236**, 21–33.
- Hipkin VJ, Voytek MA, Meyer MA, Leveille R and Domagal-Goldman SD** (2013) Analogue sites for Mars missions: NASA's Mars Science Laboratory and beyond – overview of an international workshop held at The Woodlands, Texas on March 5–6 2011. *Icarus* **224**, 261–267.
- Howard AD, Moore JM and Irwin RP** (2005) An intense terminal epoch of widespread fluvial activity on Mars: 1. Valley network incision and associated deposit. *Journal of Geophysical Research* **2110**, E12. doi: 10.1029/2005JE002459.
- Hynek BM, Osterloo MK and Kierein-Young KS** (2015) Late-stage formation of Martian chloride salts through ponding and evaporation. *Geology* **43**, 787–790. <https://doi.org/10.1130/G36895.1>
- Joshi MP, Samanta A, Tripathy GR and Rajamani S** (2017) Formation and stability of prebiotically relevant vesicular systems in terrestrial geothermal environments. *Life* **7**, 1–14.
- Jouzel J, Petit JR, Souchez R, Barkov NI, Lipenkov VY, Raynaud D, Stevenard M, Vassiliev NI, Verbeke V and Vimeux F** (1999) More than 200 meters of lake ice above subglacial Lake Vostok, Antarctica. *Science* **286**, 2138–2141.
- Kaplan HH, Milliken RE, Knoll AH, Bristow T and Knowlton ME** (2014) Detection of Organic Matter in Ancient Sedimentary Rocks Using Reflectance Spectroscopy. 45th Lunar and Planetary Science Conference. #1995.
- Kleber M, Mikutta R, Torn MS and Jahn R** (2005) Poorly crystalline mineral phases protect organic matter in acid subsoil horizons. *European Journal of Soil Science* **56**, 717–725.
- Klein HP, Horowitz NH, Levin GV, Oyama VI, Lederberg J, Rich A, Hubbard JS, Hobby GL, Straat PA, Berdahl BJ, Carle GC, Brown FS and Johnson RD** (1976) The viking biological investigation: preliminary results. *Science* **194**, 99–105.
- Kluiving SJ, Bartek LR and Van der Wateren FM** (1999) *Annals of Glaciology* **28**, 90–96.
- Kramer M, Kotlia BS and Wünnemann B** (2014) A late quaternary ostracod record from the Tso Kar basin (North India) with a note on the distribution of recent species. *Journal of Paleolimnology* **51**, 549–565. DOI: 10.1007/s10933-014-9773-7.
- Kumar S, Bora S and Sharma UK** (2016) Geological appraisal of Ladakh and Tirit Granitoids in the Indus-Shyok Suture Zones of Northwest Himalaya, India. *Journal Geological Society of India* **87**, 737–746.
- Manga M, Patel A, Dufek J and Kite ES** (2012) Wet surface and dense atmosphere on early Mars suggested by the bomb sag at Home Plate, Mars. *Geophysical Research Letters* **39**, L01202. doi: 10.1029/2011GL050192.
- McGuirk SL, Clarke J, Strong CL and Mills F** (2018) The remote sensing of valley winds in Northern Himalaya. 18th Australian Space Research Conference Proceedings, Gold Coast, Queensland, Australia, September 24–26, 2018.
- Milliken RE and Bish DL** (2010) Sources and sinks of clay minerals on Mars. *Philosophical Magazine* **90**, 2293–2308.
- Nag D and Phartiyal B** (2015) Climatic variations and geomorphology of the Indus River valley, between Nimo and Batalik, Ladakh (NW Trans Himalayas) during Late Quaternary. *Quaternary International* **371**, 87–101.
- Navarro-González R, Vargas E, de la Rosa J, Raga AC and McKay CP** (2010) Reanalysis of the Viking results suggests perchlorate and organics at mid-latitudes on Mars. *Journal of Geophysical Research* **115**, 1–11.
- Orgel LE** (2004) Prebiotic chemistry and the origin of the RNA world. *Critical Reviews in Biochemistry and Molecular Biology* **39**, 99–123.
- Osterloo MM, Hamilton VE, Bandfield JL, Glotch TD, Baldrige AM, Christensen PR, Tornabene LL and Anderson FS** (2008) Chloride-bearing materials in the southern highlands of Mars. *Science* **319**, 1651–1654. doi: 10.1126/science.1150690.
- Osterloo MM, Anderson FS, Hamilton VE and Hynek BM** (2010) Geologic context of proposed chloride-bearing materials on Mars. *Journal of Geophysical Research* **115**, E10012. doi: 10.1029/2010JE003613
- Pain CF** (2008) Field Guide for Describing Regolith and Landforms CRC LEME, c/o CSIRO Exploration and Mining, PO Box 1130, Bentley WA 6102, Australia, 94pp.
- Pain CF, Chan R, Craig M, Gibson D, Kilgour P and Wilford J** (2007) RTMAP Regolith Database Field Book and Users Guide (Second Edition). CRC LEME Open File Report 231, 92pp. (available from <http://crlcme.org.au/Pubs/reportsother.html>).
- Pant RK, Phadtare NR, Chamyal LS and Juyal N** (2005) Quaternary deposits in Ladakh and Karakoram Himalaya: a treasure trove of the palaeoclimate records. *Current Science* **88**, 1989–1798.
- Phartiyal B and Sharma A** (2009) Soft-sediment deformation structures in the Late Quaternary sediments of Ladakh: evidence for multiple phases of seismic tremors in the North-western Himalayan Region. *Journal of Asian Earth Sciences* **34**, 761–770.
- Phartiyal B, Sharma A and Kothyari GC** (2013) Damming of River Indus during Late Quaternary in Ladakh Region of Trans-Himalaya, NW India: implications to Lake formation-climate and tectonics. *Chinese Science Bulletin* **58**(Suppl. I), 142–155.
- Phartiyal B, Singh R and Nag D** (2014) Trans and Tethyan Himalayan Rivers-in reference to Ladakh and Lahaul Spiti, NW Himalaya, India. In Singh DS (ed). *The Indian Rivers: An Introduction for Science and Society*. Lucknow, India: University of Lucknow Press, pp. 266–279.
- Phartiyal B, Singh R and Kothyari GC** (2016) Late-quaternary geomorphic scenario due to changing depositional regimes in the Tangtse Valley, Trans-Himalaya, NW India. *Paleogeography, Paleoclimatology, Paleocology* **422**, 11–24.
- Philip G and Mazari RK** (2000) Shrinkinglake basins in the proximity of the Indus Suture Zone of northwestern Himalaya: a case study of Tso Kar and Startsapuk Tso, using IRS-1C data. *International Journal of Remote Sensing* **21**, 2973–2984.
- Preston LJ and Dartnell LR** (2014) Planetary habitability: lessons learned from terrestrial analogues. *International Journal of Astrobiology* **13**, 81–98.
- Saxena VK and D'Amore F** (1984) Aquifer chemistry of the Puga and Chumatang high temperature geothermal systems in India. *Journal of Volcanology and Geothermal Research* **21**, 333–346.
- Schiffman P, Howard JS, Southard RJ and Swanson DA** (2000) Controls on palagonitization versus pedogenic weathering of basaltic tephra: evidence from the consolidation and geochemistry of the Keanakako'i Ash Member, Kilauea volcano. *Geochemistry Geophysics Geosystems* **1**, 2000GC000068.
- Schubotz F, Hays LE, D'Arcy R, Gillespie A, Shock EL and Summons RE** (2015) Stable isotope labelling confirms mixotrophic nature of streamer

- biofilm communities at alkaline hot springs. *Frontiers in Microbiology* **6**, 1–6.
- Sekar B, Rajagopalan G and Bhattacharyya A** (1994) Chemical analysis and ^{14}C dating of a sediment core from Tsokar lake, Ladakh and its implication on climatic changes. *Current Science* **67**, 36–39.
- Shankar R, Padhi RN, Prakash G, Thussu JL and Wangdus C** (1976) Recent geological studies in upper Indus valley and the plate tectonics. *Geological Survey of India* **34**, 41–56.
- Shukla AD, Ray D and Bhattacharya S** (2017) Sulphate Mineral from Hot Springs in Cold Desert (Ladakh, India): Analogue to Martian Sulphate Deposit? Lunar and Planetary Science (XLVIII) Conference, March 2017, Houston, TX, USA
- Singh UK, Tiwari RK and Singh SB** (2005) One-dimensional inversion of geo-electrical resistivity sounding data using artificial neural networks – a case study. *Computers Geosciences* **31**, 99–108.
- Singh UK, Tiwari RK and Singh SB** (2010) Inversion of 2-D DC resistivity data using rapid optimization and minimal complexity neural network. *Nonlinear Processes in Geophysics* **17**, 65–76.
- Squyres SW** (2004) The opportunity Rover's athena science investigation at Meridiani Planum, Mars. *Science* **306**, 1698–1703.
- Szostak JW, Bartel DP and Luisi PL** (2001) Synthesizing life. *Nature* **409**, 387–390. doi: 10.1038/35053176.
- Thakur VC** (1981) Regional framework and Geodynamic evolution of the Indus-Tsangpo Suture Zone in the Ladakh Himalaya. *Transactions of Royal Society of Edinburgh: Earth Sciences* **72**, 89–97.
- Thakur VC** (1992) *Geology of Western Himalaya*. Oxford, UK: Pergamon Press, 366p.
- Thanh NX, Itaya T, Ahmad T, Kojima S, Ohtani T and Ehiro M** (2010) Mineral chemistry and K–Ar ages of plutons across the Karakoram fault in the Shyok-Nubra confluence of northern Ladakh Himalaya, India. *Gondwana Research* **17**, 180–188.
- Thomson BJ, Bridges NT, Milliken R, Baldrige A, Hook SJ, Crowley JK, Marion GM, de Souza Filho CR, Brown AJ and Weitz CM** (2011) Constraints on the origin and evolution of the layered mound in Gale Crater, Mars using Mars Reconnaissance Orbiter data. *Icarus* **214**, 413–443.
- Webb P-N, Ronan TE, Lipps JH and DeLaca** (1979) *Science* **203**, 435–437.
- Weinberg RF, Dunlap WJ and Whitehouse M** (2000) Newfield structural and geochronological data from the Shyok and Nubra valleys, northern Ladakh: linking Kohistan to Tibet. *Geological Society of London. Special Publication* **170**, 253–275.
- Wünnemann B, Reinhardt C, Kotlia BS and Riedel F** (2008) Observations on the relationship between lake formation, permafrost activity and lithalsal development during the last 20,000 years in the Tso Kar basin, Ladakh, India. *Permafrost and Periglacial Processes* **19**, 341–358.
- Wünnemann B, Demske D, Tarasov P, Kotlia BS, Reinhardt C, Bloemendal J, Diekmann B, Hartmann K, Krois J, Riedel F and Arya N** (2010) Hydrological evolution during the last 15kyr in the Tso Kar lake basin (Ladakh, India), derived from geomorphological, sedimentological and palynological records. *Quaternary Science Reviews* **29**, 1138–1155.
- Yu G, Harrison SP and Xue B** (2001) Lake status records from China: Data Base Documentation. MPI-BGC Technical report 4.
- Yu B, Dong H, Jiang H, Guo LV, Eberl D, Li S and Kim J** (2009) “The role of clay minerals in the preservation of organic matter in sediments of Qinghai Lake, NW China. Clays and Clay Minerals.” The role of clay minerals in the preservation of organic matter in sediments of Qinghai Lake, NW China. *Clays and Clay Minerals* **57**, 213–26.
- Zotikov IA and Jacobs S** (1985) Oceanic inclusions in the J-9 sea ice core. *Antarctic Journal of the USA* **20**, 113–115.